

Stochastic tree ensembles for regularized nonlinear regression

Jingyu He
City University of Hong Kong
and
P. Richard Hahn
Arizona State University

November 4, 2021

Abstract

This paper develops a novel stochastic tree ensemble method for nonlinear regression, referred to as Accelerated Bayesian Additive Regression Trees, or XBART. By combining regularization and stochastic search strategies from Bayesian modeling with computationally efficient techniques from recursive partitioning algorithms, XBART attains state-of-the-art performance at prediction and function estimation. Simulation studies demonstrate that XBART provides accurate point-wise estimates of the mean function and does so faster than popular alternatives, such as BART, XGBoost, and neural networks (using Keras) on a variety of test functions.

Additionally, it is demonstrated that using XBART to initialize the standard BART MCMC algorithm considerably improves credible interval coverage and reduces total run-time.

Finally, three basic theoretical results are established: 1) the single tree version of the model is asymptotically consistent, 2) samples obtained from the single-tree version of the algorithm correspond to posterior samples under a particular likelihood and prior specification, and 3) the Markov chain produced by the ensemble version of the algorithm has a unique stationary distribution.

Keywords: Machine learning; Markov chain Monte Carlo; Regression trees; Supervised learning; Bayesian

1 Introduction

Tree-based algorithms for supervised learning, such as Classification and Regression Trees (CART) ([Breiman et al., 1984](#)), random forests ([Breiman, 2001](#)) and boosted regression trees ([Friedman, 2002](#); [Chen and Guestrin, 2016](#)), are popular due to their speed and accuracy in out-of-sample prediction tasks. For instance, in section 10.7 of [Hastie et al. \(2005\)](#), an influential textbook, we read

Of all the well-known learning methods, decision trees come closest to meeting the requirements for serving as an off-the-shelf procedure for data mining. They are relatively fast to construct and they produce interpretable models (if the trees are small). They naturally incorporate mixtures of numeric and categorical predictor variables and missing values. They are invariant under (strictly monotone) transformations of the individual predictors. As a result, scaling and/or more general transformations are not an issue, and they are immune to the effects of predictor outliers. They perform internal feature selection as an integral part of the procedure. They are thereby resistant, if not completely immune, to the inclusion of many irrelevant predictor variables. These properties of decision trees are largely the reason that they have emerged as the most popular learning method for data mining. Trees have one aspect that prevents them from being the ideal tool for predictive learning, namely inaccuracy. They seldom provide predictive accuracy comparable to the best that can be achieved with the data at hand. Boosting decision trees improves their accuracy, often dramatically.

In 2016, the XGBoost algorithm was introduced ([Chen and Guestrin, 2016](#)) and has quickly become a go-to tool for data scientists working in industry:

Take the challenges hosted by the machine learning competition site Kaggle for example. Among the 29 challenge winning solutions 3 published at Kaggle’s blog during 2015, 17 solutions used XGBoost. Among these solutions, eight solely used XGBoost to train the model, while most others combined XGBoost with neural nets in ensembles. For comparison, the second most popular method, deep neural nets, was used in 11 solutions. The success of the system was also witnessed in KDDCup 2015, where XGBoost was used by every winning team in the top 10 ([Bekkerma, 2015](#)).

[Pafka \(2015\)](#) performed simulation comparisons of the performance of XGBoost and other gradient boosting methods and random forests, and conclude that XGBoost is fast, memory efficient and of high accuracy. [Brownlee \(2016\)](#) summarizes insightful quotes and praises

from Kaggle competition winners on XGBoost.

At the same time, an older tree-based method, random forests ([Breiman, 2001](#)), is often faster and competitively accurate, especially on low-signal data sets. In Section 15.2 of *Elements of Statistical Learning* [Hastie et al. \(2005\)](#), the authors remark:

In our experience random forests do remarkably well, with very little tuning required.

In short, it would not be much of an exaggeration to say that XGBoost and random forests are the standard bears for classification and regression problems with the unstructured (tabular) mixed numeric-categorical data that is common in many industries.

Still, there may be room for improvement, in at least two respects. One, it would be preferable to have a single method that could replace the two, a method that works well on both high and low signal data sets. To some extent XGBoost can avoid overfitting, and hence achieve model fits more like random forests, by choosing a less aggressive learning rate (one of the algorithms tunable parameters), but selecting this parameter by cross-validation can be costly, essentially undoing the tremendous speed advantage for which XGBoost is famous. Two, in some situations it would be useful to have a prediction interval in addition to a point estimate. Although some approaches, such as conformal prediction ([Lei et al., 2018](#)), can be used to augment XGBoost or random forests, doing so comes at a steep computational cost. In these two respects — regularization that is adaptive to problem difficulty (data quality) and availability of an associated uncertainty measure — a third popular tree ensemble method arises as a competitor: Bayesian additive regression trees (BART) ([Chipman et al., 2010](#)) is a model-based method that is comparatively robust to the choice of tuning-parameters and, as a Bayesian method, provides posterior uncertainty quantification. Due to these strengths, BART has inspired a considerable body of research in recent years; for a comprehensive review of this literature, see [Linero \(2017\)](#) and [Hill et al. \(2020\)](#).

However, relative to random forests and XGBoost, BART models take much longer to fit because the underlying random walk Metropolis-Hastings Markov chain Monte Carlo (MCMC) algorithm can be slow to converge. The present paper develops a novel stochastic tree ensemble method, referred to as Accelerated Bayesian Additive Regression Trees, or

XBART, that greatly reduces the time needed to fit BART models. XBART takes its regularization and parameter sampling steps from BART, while retaining the recursive tree-growing process from traditional tree-based methods. The result is a stochastic tree sampling algorithm that is substantially faster than BART while retaining its state-of-the-art predictive accuracy. A general form of the recursive stochastic algorithm is presented in Section 2; Section 3 tailors the algorithm to a regression model with additive Gaussian errors. Extensive simulation studies and empirical data examples demonstrate the efficacy of the new approach in Section 4.

Furthermore, XBART works not only as a stand-alone machine learning algorithm but can be used to initialize a BART MCMC sampler (warm-start BART, Section 5), resulting in faster fully Bayesian inference with improved posterior exploration as indicated by posterior credible intervals (for the mean function) with better coverage (for a fixed number of posterior samples).

Finally, basic theoretical properties of the new algorithm are investigated in Section 6. First, recent consistency results concerning CART and random forests (Scornet et al., 2015) are shown to apply to XBART with a single tree. Second, it is shown that the XBART forest algorithm defines a finite-space Markov chain with stationary distribution.

The XBART algorithm was first presented in He et al. (2019); relative to this initial description, the version of XBART presented here is expressed in more generality, the simulation studies are more extensive, and the real data examples, the warm-start strategy and the theoretical results are entirely new.

2 A recursive, stochastic fitting algorithm

The goal of supervised learning is to predict a scalar random variable $Y \in \mathcal{Y}$ by a length p covariate vector $\mathbf{x} = (x_1, \dots, x_p) \in \mathcal{X}$. This section presents a stochastic, recursive algorithm for supervised learning with decision or regression trees. The algorithm is first developed for fitting a single tree and then extended to tree ensembles, or forests. This section describes the algorithm in terms that apply to a general likelihood function that can be used for classification or regression; the remainder of the paper focuses on regression

with a continuous univariate response variable.

2.1 Fitting a single tree recursively and stochastically

A tree T is a set of split rules defining a rectangular partition of the covariate space to $\{\mathcal{A}_1, \dots, \mathcal{A}_B\}$, where B is the total number of terminal nodes of tree T . The split rule is a pair of (x_i, c) , indicating variable to split and the value at which it cuts. Each rectangular cell \mathcal{A}_b is associated with leaf parameter μ_b and the pair $(T, \boldsymbol{\mu})$ parameterizes a step function $g(\cdot)$ on covariate space:

$$g(\mathbf{x}; T, \boldsymbol{\mu}) = \mu_b, \quad \text{if } \mathbf{x} \in \mathcal{A}_b$$

where $\boldsymbol{\mu} = (\mu_1, \dots, \mu_B)$ denotes a vector of all leaf parameters. Figure 1 depicts a simple regression tree using two variables $\mathbf{x} = (x_1, x_2) \in [0, 1] \times [0, 1]$. The left panel shows a split rule structure and the right panel plots the corresponding partition of the space and the associated leaf parameters. The response distribution at a point \mathbf{x} , upon which predictions are based, is determined by the leaf parameter, μ_b , associated with the cell containing \mathbf{x} .

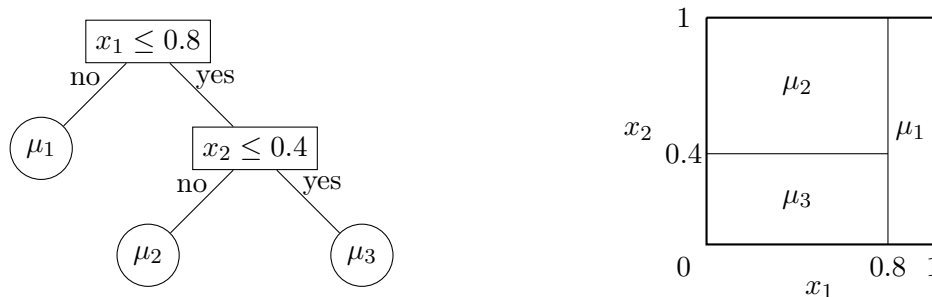


Figure 1: A regression tree on two variables depicting two split rules (cutpoints) and three leaf nodes.

Regression trees may be “grown” by recursive partitioning: the best split rule (cutpoint) is determined by examining all cutpoint candidates along each variable, where best is defined by a specified split criterion. The data set is then divided according to this split rule (cutpoint) and the process is repeated on the resulting disjoint subsets until a stopping condition is met. Algorithm 1 depicts pseudocode for recursive partitioning.

Most widely-used regression tree methods are some version of Algorithm 1, differing from one another in terms of the split criteria and stopping conditions they employ. Split

Algorithm 1 Recursive partitioning

```
1: A length- $n$  response vector  $\mathbf{y}$  and a  $n \times p$  predictor matrix  $\mathbf{X}$ .
2: procedure RECURSIVEPARTITION( $\mathcal{I}$ ) ▷ Row indices  $\mathcal{I}$ , a subset of  $1, \dots, n$ .
3:   if Stop( $\mathcal{I}$ ) = FALSE then
4:     Compute split criterion based on partitions of  $\mathbf{y}$  corresponding to each candidate cutpoint
     defined by  $\mathcal{I}$  and  $\mathbf{X}$ .
5:     Define disjoint subsets  $\mathcal{I}_{\text{left}}$  and  $\mathcal{I}_{\text{right}}$  based on the optimal cutpoint.
6:     RECURSIVEPARTITION( $\mathcal{I}_{\text{left}}$ )
7:     RECURSIVEPARTITION( $\mathcal{I}_{\text{right}}$ )
8:   else
9:     return a single prediction based on observations  $y_i$  for  $i \in \mathcal{I}$ .
10:  end if
end procedure
```

criteria are functions of a split rule (a cutpoint), measuring homogeneity within the two child nodes produced by the implied split; for instance, CART (Breiman et al., 1984) uses a squared error split criteria. Frequently used stop conditions include maximum depth of a tree, minimal number of data observations within a leaf node, or a threshold for percent change of split criteria from parent to child nodes.

The XBART algorithm is a modification of Algorithm 1 in which the partition cutpoints and also the stopping condition are determined *stochastically*. The splitting criterion will be motivated by analogy with an integrated likelihood calculation arising from the BART MCMC algorithm (Chipman et al., 2010). Here we present the result in a highly generic form; details specific to the Gaussian mean regression model are given in Section 3.

2.1.1 The XBART marginal likelihood split criterion

To establish notation: The predictor matrix \mathbf{X} , with dimension $n \times p$, consists of n observations and p variables. Tree regression methods partition the data according to predictor values, which are recorded in the predictor matrix \mathbf{X} . The set of split rule candidates, denoted \mathcal{C} , is defined by \mathbf{X} with each element indexed as c_{jk} where $j = 1, \dots, p$ indexes a variable (column) of \mathbf{X} and k indexes a set of candidate cutpoints (row) of \mathbf{X} . In this paper, we use the term *cutpoint* to refer to c_{jk} , with the understanding that the value of c_{jk} and the index j jointly define a splitting rule.

Let $|\mathcal{C}|$ denote the total number of candidate cutpoints. Let Φ denote prior hyperparameters and Ψ denote model parameters; that is, Φ is fixed during the entire process

fitting (such as prior parameters), while model parameters Ψ are to be estimated (such as residual variance for the regression case)¹.

Consider a likelihood $\ell(y_b; \mu_b, \Psi_b)$ on one leaf with leaf-specific parameter μ_b and additional model parameters Φ . In the following text, we omit subscript b for simplicity. The leaf parameter μ is given a prior $\pi(\mu; \Phi)$ and induces the prior predictive distribution

$$m(y; \Phi, \Psi) := \int \ell(y; \mu, \Psi) \pi(\mu; \Phi) d\mu, \quad (1)$$

This prior predictive distribution will define the XBART split criterion. Observe that this framework can accommodate many different models, defined by the choice of likelihood function $\ell(y; \mu, \Psi)$: it could be Gaussian for regression (Section 3), a multinomial distribution for classification, etc.

Intuitively, the split criterion arises via Bayesian estimation of a single unknown parameter, the cutpoint defining the partition (which may be null, as in the data is not to be split at all). From this “local” perspective (ignoring its implications further down the tree), the posterior probability of each candidate cutpoint is determined according to the above prior predictive distribution (equivalently, the marginal likelihood). In more detail, a cutpoint c_{jk} partitions the current node to left and right child nodes, with (sub)vectors $y_{jk}^{(1)}$ and $y_{jk}^{(2)}$, respectively. Assuming that observations in separate leaf nodes are independent, the joint prior predictive associated to this local Bayesian model is simply the product of the predictive distribution in each of the two partitions defined by c_{jk} :

$$L(c_{jk}) := m(y_{jk}^{(1)}; \Phi, \Psi) \times m(y_{jk}^{(2)}; \Phi, \Psi), \quad (2)$$

which defines the split criterion for cutpoint c_{jk} . Similarly, the *null cutpoint* is defined as

$$L(\emptyset) := |\mathcal{C}| \left(\frac{(1+d)^\beta}{\alpha} - 1 \right) m(y; \Phi, \Psi) \quad (3)$$

where d is depth of the current node and α, β are hyper-parameters. Once the split criterion has been evaluated at all candidate cutpoints (including the null cutpoint), one of them is

¹The distinction between Φ and Ψ is perhaps clearest in concrete instances of the algorithm; see section 3 for an example of Gaussian regression.

sampled with probability proportional to the split criterion value:

$$\begin{aligned} P(c_{jk}) &= \frac{L(c_{jk})}{\sum_{c_{jk} \in \mathcal{C}} L(c_{jk}) + L(\emptyset)}, \\ P(\emptyset) &= \frac{L(\emptyset)}{\sum_{c_{jk} \in \mathcal{C}} L(c_{jk}) + L(\emptyset)}. \end{aligned} \tag{4}$$

The additional weight on the null cutpoint criterion, $|\mathcal{C}| \left(\frac{(1+d)^\beta}{\alpha} - 1 \right)$, was chosen to match the tree prior used in standard BART (Chipman et al., 2010), in the following sense. Setting $m(\cdot; \Phi, \Psi) = 1$ for all cutpoints in \mathcal{C} entails that the prior probability of splitting at one of the cutpoints is

$$1 - P(\emptyset) = \frac{|\mathcal{C}|}{|\mathcal{C}| \left(\frac{(1+d)^\beta}{\alpha} - 1 \right) + |\mathcal{C}|} = \alpha(1+d)^{-\beta}.$$

Once the null cutpoint is sampled (or other stopping conditions are met), the recursion terminates, returning the leaf parameter μ , sampled from the associated “local” Bayesian posterior. Algorithm 2 presents this algorithm, which we call GROWFROMROOT. Note that Algorithm 2 expresses $m(y; \Phi, \Psi)$ in terms of a sufficient statistic $s(y)$, which can aid computation; for a concrete example see Section 3.1.

2.2 Tree ensembles

Tree ensemble prediction methods combine L decision or regression trees, T_l , $l = 1, \dots, L$ to produce a prediction function mapping $\mathcal{X} \rightarrow \mathcal{Y}$. Although the simplicity of single-tree methods such as CART have their appeal, the most accurate tree-based prediction methods are ensemble approaches: Random forests (Breiman, 2001), gradient boosting (Friedman, 2001), and BART (Chipman et al., 2010). To extend the grow-from-root algorithm to tree ensembles (or “forests”) we simply define the split criterion itself as a function of the “leave-one-out forest”. Let $\mathcal{F} = \{T_1, \dots, T_L\}$ denote the complete forest and let $\mathcal{F}_{-h} = \mathcal{F} \setminus T_h$. Similarly, let $\mathcal{M} = \{\mu_1, \dots, \mu_L\}$ denote the set of associated leaf parameters and $\mathcal{M}_{-h} = \mathcal{M} \setminus \mu_h$. One may then define a marginal likelihood as

$$m(y; \Phi, \{\Psi, \mathcal{F}_{-h}, \mathcal{M}_{-h}\}) := \int \ell(y; \mu, \{\Psi, \mathcal{F}_{-h}, \mathcal{M}_{-h}\}) \pi(\mu; \Phi) d\mu, \tag{5}$$

Algorithm 2 GrowFromRoot

1: **procedure** GROWFROMROOT($y, \mathbf{X}, \Phi, \Psi, d, T, \text{node}$)
 2: **outcome** Modifies T by adding nodes and sampling associated leaf parameters μ .
 3: **if** the stopping conditions are met **then**
 4: Go to step 15, update leaf parameter μ_{node} .
 5: **end if**
 6: $s^\emptyset \leftarrow s(y, \mathbf{X}, \Psi, \mathcal{C}, \text{all})$. \triangleright Compute sufficient statistic of stop-splitting.
 7: **for** $c_{jk} \in \mathcal{C}$ **do** \triangleright Enumerate all cutpoint candidates.
 8: $s_{jk}^{(1)} \leftarrow s(y, \mathbf{X}, \Psi, \mathcal{C}, j, k, \text{left})$. \triangleright Compute sufficient statistic of left candidate node.
 9: $s_{jk}^{(2)} \leftarrow s(y, \mathbf{X}, \Psi, \mathcal{C}, j, k, \text{right})$. \triangleright Compute sufficient statistic of right candidate node.
 10: Calculate $L(c_{jk}) = m\left(s_{jk}^{(1)}; \Phi, \Psi\right) \times m\left(s_{jk}^{(2)}; \Phi, \Psi\right)$
 11: **end for**
 12: Calculate $L(\emptyset) = |\mathcal{C}| \left(\frac{(1+d)^\beta}{\alpha} - 1 \right) m(s^\emptyset; \Phi, \Psi)$.
 13: Sample a cutpoint c_{jk} proportional to integrated likelihoods

$$P(c_{jk}) = \frac{L(c_{jk})}{\sum_{c_{jk} \in \mathcal{C}} L(c_{jk}) + L(\emptyset)},$$

$$\text{or } P(\emptyset) = \frac{L(\emptyset)}{\sum_{c_{jk} \in \mathcal{C}} L(c_{jk}) + L(\emptyset)} \text{ for the null cutpoint.}$$

14: **if** the null cutpoint is selected **then**
 15: $\mu_{\text{node}} \leftarrow \text{SampleParameters}(s^\emptyset)$
 16: **return**.
 17: **else**
 18: Create two new nodes, **left_node** and **right_node**, and grow T by designating them as the current node's (**node**) children.
 19: Partition the data (y, \mathbf{X}) into left $(y_{\text{left}}, \mathbf{X}_{\text{left}})$ and right $(y_{\text{right}}, \mathbf{X}_{\text{right}})$ parts, according to the selected cutpoint $x_{ij'} \leq x_{kj}^*$ and $x_{ij'} > x_{kj}^*$, respectively, where x_{kj}^* is the value corresponding to the sampled cutpoint c_{jk} .
 20: GROWFROMROOT($y_{\text{left}}, \mathbf{X}_{\text{left}}, \Phi, \Psi, d+1, T, \text{left_node}$).
 21: GROWFROMROOT($y_{\text{right}}, \mathbf{X}_{\text{right}}, \Phi, \Psi, d+1, T, \text{right_node}$).
 22: **end if**
 23: **end procedure**

provided the integral is well-defined. In this formulation, GROWFROMROOT may be conceptualized in terms of a Bayesian model with all but the h -th tree known (including the associated leaf parameters). This is much like specifying a model in terms of full conditional distributions; in general this will not yield a stationary distribution, but in Section 6.2 we show that XBART does. In the case of additive ensembles for mean regression with additive Gaussian errors, these expressions are particularly convenient (see Section 3).

The XBART stochastic ensemble method is detailed in Algorithm 3. It produces I samples of the forest \mathcal{F} . We refer to one iteration of the algorithm, sampling all L trees once, as a *sweep*. Additional (model-specific) parameters, Ψ , are updated in between sampling each tree (for a total of L updates per sweep), or in between sampling each forest (one update per sweep), depends on the parameter.

Algorithm 3 Accelerated Bayesian Additive Regression Trees (XBART)

```

1: procedure XBART( $y, \mathbf{X}, \Phi, L, I$ )
2: output  $I$  posterior draws of a forest (and associated leaf parameters) comprising  $L$  trees.
3:   Initialize  $\Psi$  and all  $T_h$ , for  $h = 1, \dots, L$ .
4:   for  $iter$  in 1 to  $I$  do
5:     for  $h$  in 1 to  $L$  do
6:       Create new_node.
7:       Initialize tree  $T_h^{(iter)}$  to the root node.
8:       GROWFROMROOT( $y, \mathbf{X}, \{\Psi, \mathcal{F}_{-h}, \mathcal{M}_{-h}\}, \Phi, T_h^{(iter)}, \mathbf{new\_node}$ ).
9:       Sample some elements of  $\Psi$ , in between of each tree.
10:    end for
11:    Sample some elements of  $\Psi$ , in between of each sweep.
12:  end for
13: end procedure

```

3 Regression with XBART

This section derives the specific forms of the split criterion and the parameter sampling distributions corresponding to a homoskedastic Gaussian additive error model:

$$\begin{aligned}
Y &= f(\mathbf{x}) + \epsilon, \\
&= \sum_{l=1}^L g(\mathbf{x}; T_l, \boldsymbol{\mu}_l) + \epsilon,
\end{aligned} \tag{6}$$

where f is a unknown mean function that is represented as a sum of regression trees, $f(\mathbf{x}) = \mathbb{E}[Y \mid \mathbf{x}]$, and $\epsilon \sim \mathcal{N}(0, \sigma^2)$. The additional non-tree parameters in this case are the residual variance and the common prior variance over the leaf means: $\Psi := (\sigma^2, \tau)$, which are given inverse-Gamma(a_σ, b_σ) and inverse-Gamma(a_τ, b_τ) priors, respectively. Parameter σ^2 is updated between tree updates while τ is updated between sweeps.

Reviewing notation, $\mathbf{x}_i = (x_{i1} \cdots, x_{ip})$ is the i -th observation of a p dimensional covariate (row) vector and $y \in \mathbb{R}$ is the real response variable. Capital letter Y denote the response variable considered as a random variable, whereas $\mathbf{y} = (y_1, \cdots, y_n)$ denotes a length n vector of corresponding realized data observations, and $\mathbf{X} = (\mathbf{x}_1^t, \cdots, \mathbf{x}_n^t)^t$ is a $n \times p$ matrix of covariate data, where rows are observations and columns are features. Leaf parameters are given independent and identical Gaussian priors, $\mu \sim \mathcal{N}(0, \tau)$. In the notation of section 2.1, these modeling choices correspond to hyper-parameter $\Phi = \{a_\sigma, b_\sigma, a_\tau, b_\tau\}$ and model parameter $\Psi = \{\sigma, \tau\}$, respectively.

3.1 Sampling cutpoints

This section dervies the explicit form of split criterion for the Gaussian regression case, which corresponds to line 6 to 13 in Algorithm 2.

Proposition 1. *For the Gaussian regression case, the split criterion for a cutpoint candidate c_{jk} and the null cutpoint in equation (2) and (3) has the specific form as*

$$\begin{aligned} L(c_{jk}) &\propto \exp \left[\frac{1}{2} \sum_{b=1}^2 \left(\log \left(\frac{\sigma^2}{\sigma^2 + \tau n_{jk}^{(b)}} \right) + \frac{\tau}{\sigma^2(\sigma^2 + \tau n_{jk}^{(b)})} (s_{jk}^{(b)})^2 \right) \right], \\ L(\emptyset) &\propto |\mathcal{C}| \left(\frac{(1+d)^\beta}{\alpha} - 1 \right) \times \exp \left[\frac{1}{2} \left(\log \left(\frac{\sigma^2}{\sigma^2 + \tau n} \right) + \frac{\tau}{\sigma^2(\sigma^2 + \tau n)} s(\mathbf{y})^2 \right) \right]. \end{aligned} \quad (7)$$

Here, suppose there are n data observations in the current node, and the cutpoint candidate c_{jk} partitions data to left and right child nodes, with $n_{jk}^{(1)}$ and $n_{jk}^{(2)}$ observations in each, and $n_{jk}^{(1)} + n_{jk}^{(2)} = n$. Let $s_{jk}^{(1)} = \sum_{i \in \text{left child}} y_i$, $s_{jk}^{(2)} = \sum_{i \in \text{right child}} y_i$ denote the sufficient statistics of data in the two child nodes. Let $s(\mathbf{y}) = s_{jk}^{(1)} + s_{jk}^{(2)} = \sum_{i=1}^n y_i$ denote the sufficient statistics of all the data observations. The notation $|\mathcal{C}|$ indicates number of cutpoint candidates in total.

Remark Expressions (8) are denoted up to proportionality because any constants cancel when normalizing the probabilities in equation (4). Because the XBART regression split criterion depends on a sufficient statistic only, it can be computed rapidly if the data are pre-sorted, see Appendix A for details regarding computational considerations.

Proof. We first describe the marginal likelihood criteria assuming a single tree. Assuming that observations in the same leaf node share are independent and identically distributed, the prior predictive distribution of equation (2) is simply a mean-zero multivariate Gaussian distribution,

$$\begin{aligned} m(y; \tau, \sigma) &= \int \phi(y; \mu \mathbf{J}_n, \sigma^2 \mathbf{I}_n) \phi(\mu; 0, \tau) d\mu = \phi(0, \Omega) \\ &= (2\pi)^{-n/2} \det(\Omega)^{-1/2} \exp\left(-\frac{1}{2} y^t \Omega^{-1} y\right), \end{aligned} \quad (8)$$

with covariance matrix and corresponding inverse

$$\Omega = \tau \mathbf{J}_n \mathbf{J}_n^t + \sigma^2 \mathbf{I}_n, \quad \Omega^{-1} = \sigma^{-2} \mathbf{I}_n - \frac{\tau}{\sigma^2(\sigma^2 + \tau n)} \mathbf{J}_n \mathbf{J}_n^t.$$

Here \mathbf{J}_n is a length n column vector of all ones; \mathbf{I}_n is a n dimensional identity matrix; $\phi(y; \mu \mathbf{J}_n, \sigma^2 \mathbf{I}_n)$ denotes the likelihood, density of multivariate Gaussian distribution with mean $\mu \mathbf{J}_n$ and covariance matrix $\sigma^2 \mathbf{I}_n$; $\phi(\mu; 0, \tau)$ is the density of the univariate Gaussian prior over μ ; and n is number of data observations comprising y .

The prior predictive density of equation (8) may be simplified as follows. First, apply Sylvester's determinant theorem to $\det \Omega^{-1}$:

$$\det \Omega^{-1} = \sigma^{-2n} \left(1 - \frac{\tau n}{\sigma^2 + \tau n}\right) = \sigma^{-2n} \left(\frac{\sigma^2}{\sigma^2 + \tau n}\right).$$

Taking logarithms of the density in equation (8) yields

$$-\frac{n}{2} \log(2\pi) - n \log \sigma - \frac{1}{2} \frac{y^t y}{\sigma^2} + \frac{1}{2} \log\left(\frac{\sigma^2}{\sigma^2 + \tau n}\right) + \frac{1}{2} \frac{\tau}{\sigma^2(\sigma^2 + \tau n)} s(y)^2,$$

with

$$s(y) = y^t \mathbf{J} = \sum_{i=1}^n y_i, \quad s(y)^2 = y^t \mathbf{J} \mathbf{J}^t y = \left(\sum_{i=1}^n y_i\right)^2.$$

Assume the cutpoint c_{jk} partitions the data into left and right child nodes according to the

split rule $\{x_j \leq c_{jk}\}$ and $\{x_j > c_{jk}\}$. Denote the response (sub)vectors in left and right child nodes as $y_{jk}^{(1)}, y_{jk}^{(2)}$ of length $n_{jk}^{(1)}$ and $n_{jk}^{(2)}$, respectively. The (log) marginal likelihood for cutpoint c_{jk} is then

$$\begin{aligned} & \log \left[m \left(s_{jk}^{(1)}; \tau, \sigma \right) \times m \left(s_{jk}^{(2)}; \tau, \sigma \right) \right] \\ &= \sum_{b=1}^2 -\frac{n_{jk}^{(b)}}{2} \log(2\pi) - n_{jk}^{(b)} \log \sigma - \frac{1}{2} \frac{\left(y_{jk}^{(b)} \right)^t y_{jk}^{(b)}}{\sigma^2} + \frac{1}{2} \log \left(\frac{\sigma^2}{\sigma^2 + \tau n_{jk}^{(b)}} \right) + \frac{1}{2} \frac{\tau}{\sigma^2(\sigma^2 + \tau n_{jk}^{(b)})} \left(s_{jk}^{(b)} \right)^2 \quad (9) \\ &= -\frac{n}{2} \log(2\pi) - n \log(\sigma) - \frac{1}{2} \frac{y^t y}{\sigma^2} + \frac{1}{2} \sum_{b=1}^2 \left[\log \left(\frac{\sigma^2}{\sigma^2 + \tau n_{jk}^{(b)}} \right) + \frac{\tau}{\sigma^2(\sigma^2 + \tau n_{jk}^{(b)})} \left(s_{jk}^{(b)} \right)^2 \right], \end{aligned}$$

where the summation runs over the two child nodes created by c_{jk} , and $s_{jk}^{(1)}$ and $s_{jk}^{(2)}$ denote the sufficient statistics of the respective partitions, specifically

$$s_{jk}^{(1)} = s(y_{jk}^{(1)}), \quad s_{jk}^{(2)} = s(y_{jk}^{(2)}), \quad s_{jk}^{(1)} + s_{jk}^{(2)} = \sum_{i=1}^n y_i = s(y).$$

Noting that the first three terms of equation (9) are unaffected by the cutpoint c_{jk} , but just rely on all data observations in the current node. Thus they may be ignored, yielding split criterion for cutpoint c_{jk} :

$$\begin{aligned} L(c_{jk}) &= m \left(s_{jk}^{(1)}; \tau, \sigma \right) \times m \left(s_{jk}^{(2)}; \tau, \sigma \right) \\ &\propto \exp \left[\frac{1}{2} \sum_{b=1}^2 \left(\log \left(\frac{\sigma^2}{\sigma^2 + \tau n_{jk}^{(b)}} \right) + \frac{\tau}{\sigma^2(\sigma^2 + \tau n_{jk}^{(b)})} \left(s_{jk}^{(b)} \right)^2 \right) \right]. \end{aligned}$$

Furthermore, we denote $l(c_{jk}) = \log(L(c_{jk}))$ in the remainder of the paper. Similarly, following equation (3), the null cutpoint criterion is calculated according to

$$L(\emptyset) \propto |\mathcal{C}| \left(\frac{(1+d)^\beta}{\alpha} - 1 \right) \times \exp \left[\frac{1}{2} \left(\log \left(\frac{\sigma^2}{\sigma^2 + \tau n} \right) + \frac{\tau}{\sigma^2(\sigma^2 + \tau n)} s(y)^2 \right) \right].$$

□

Finally, observe that the XBART split criterion involves the (current estimate of the) residual standard error σ , thereby providing adaptive regularizing. The role of σ in the split criterion vanishes asymptotically (see Section 6.1.2 expression 13), but the algorithm's finite sample performance depends on the specific value, providing adaptive regularization.

3.1.1 The ensemble case

In the case of multiple trees, XBART “residualizes” the data with respect to the partial fit corresponding to the partial forest \mathcal{F}_{-h} . Formally,

$$\begin{aligned} m(y; \tau, \{\sigma, \mathcal{F}_{-h}, \mathcal{M}_{-h}\}) &= \int \phi(y; f_{-h}(x) + \mu \mathbf{J}_n, \sigma^2 \mathbf{I}_n) \phi(\mu; 0, \tau) d\mu \\ &= m(y - f_{-h}(\mathbf{X}); \tau, \sigma) \end{aligned} \tag{10}$$

where

$$f_{-h}(\mathbf{X}) = \sum_{l \neq h} g(\mathbf{X}; T_l, \boldsymbol{\mu}_l)$$

and $g(\cdot)$ is applied row-wise to \mathbf{X} . According to this specification, the split criterion may be computed as described above, simply replacing response y by the residual $y - f_{-h}(\mathbf{X})$ in expressions (7). Such “residualization” is analogous to the “Bayesian back-fitting” procedure described in [Chipman et al. \(2010\)](#). Appendix B demonstrates a simple example of fitting and residualization of a three-tree forest.

3.2 Parameter sampling

This section introduces sampling steps for leaf-specific parameters as well as global model parameters for the Gaussian regression model, corresponding to step 15 in Algorithm 2 and line 9, line 11 in Algorithm 3.

3.2.1 Leaf parameter sampling

In the GrowFromRoot Algorithm 2, once the null cutpoint is sampled, or other stopping conditions are satisfied, the current partition \mathcal{A}_{lb} is designated as the b -th leaf of l -th tree and its associated leaf parameter μ_{lb} is sampled in step 15 of Algorithm 2. Assuming a conjugate Gaussian prior, $\mu_{lb} \sim N(0, \tau)$, yields the following conjugate “full conditional” (given the current partial fit f_{-h}):

$$\mu_{lb} \sim N\left(\frac{s_{lb}}{\sigma^2\left(\frac{1}{\tau} + \frac{n_{lb}}{\sigma^2}\right)}, \frac{1}{\frac{1}{\tau} + \frac{n_{lb}}{\sigma^2}}\right),$$

where n_{lb} is number of data observations in the node and $s_{lb} = \sum_{x_i \in \mathcal{A}_{lb}} (y_i - f_{-h}(x_i))$.

3.2.2 Global parameter sampling

Next, consider the global (non-tree-specific) model parameter sampling step (line 9, line 11) of Algorithm 3. For Gaussian regression model (6), we sample the residual variance σ^2 and prior variance τ . First, the residual variance σ^2 updates in between of each tree (line 9 of Algorithm 3). Assuming a conjugate inverse-Gamma prior, $\sigma^2 \sim \text{inverse-Gamma}(a_\sigma, b_\sigma)$, the corresponding ‘‘full conditional’’ is

$$\sigma^2 \sim \text{inverse-Gamma}(n + a_\sigma, \mathbf{r}^t \mathbf{r} + b_\sigma),$$

where $\mathbf{r} = \mathbf{y} - f(\mathbf{X})$ is the vector of residuals based on the current fit

$$f(\mathbf{X}) = \sum_{l=1}^L g(\mathbf{X}; T_l, \boldsymbol{\mu}_l),$$

where $g(\cdot)$ is applied row-wise to \mathbf{X} .

The prior variance of the leaf parameter τ is assumed similar conjugate inverse-Gamma prior, $\tau \sim \text{inverse-Gamma}(a_\tau, b_\tau)$. Based on extensive experiments, we prefer sampling τ in between of each sweep (line 11 of Algorithm 3) rather than each tree, since a single tree can be shallow and do not have enough leaf parameters to update τ . Suppose μ_{lb} is the b -th leaf of the l -th tree, $\tilde{\boldsymbol{\mu}} = \{\mu_{lb}\}_{1 \leq l \leq L, 1 \leq b \leq B_l}$ being the collection of all leaf parameters of the L trees in the forest, and $|\tilde{\boldsymbol{\mu}}|$ being counts of elements in the set. The corresponding sampling distribution is

$$\tau \sim \text{inverse-Gamma} \left(|\tilde{\boldsymbol{\mu}}| + a_\tau, \sum_{\mu_{lb} \in \tilde{\boldsymbol{\mu}}} \mu_{lb}^2 + b_\tau \right).$$

Based on our extensive simulation studies, we recommend setting $a_\tau = 3$ and $b_\tau = 0.5 \times \text{Var}(y)/L$ as the default choice of the hyper-parameters.

3.3 Prediction

Predictions are obtained from XBART by taking posterior point-wise averages as if the sampled trees were draws from a standard Bayesian Monte Carlo algorithm. That is, given I iterations of the algorithm, the final $I - I_0$ samples are used to compute a point-wise average function evaluation, where $I_0 < I$ denotes the length of the burn-in period. We recommend $I = 40$ and $I_0 = 15$ for routine use. The final estimator is therefore expressed as

$$\hat{y}_i = \bar{f}(x_i) = \frac{1}{I - I_0} \sum_{k > I_0}^I f^{(k)}(x_i).$$

where $f^{(k)}$ denotes the k -th iteration of Algorithm 3. This point-wise mean estimator corresponds to the Bayes optimal estimator under mean squared error estimation loss if we were to regard our samples as coming from a traditional posterior distribution. As the GROWFROMROOT sampler is not a proper full conditional, this estimator must be considered an approximation of some sort. Nonetheless, simulation results strongly suggest that the approximation is adequate, as described in the following section. Importantly, the recursive nature of XBART enables us to employ many computational strategies that cannot be applied to BART MCMC; see the Appendix A for a description of these strategies. Section 5 describes how to use XBART to improve the posterior exploration of BART MCMC for fully Bayesian inference and Section 6 provides some preliminary theory pertaining to the above XBART point estimator.

4 Demonstrations

This section documents the favorable empirical performance of XBART relative to other popular nonlinear regression methods. Results on synthetic data are presented first, followed by results on a number of publicly available real-world data sets.

Here, our comparisons focus on XGBoost (Chen and Guestrin, 2016) and random forests (Breiman, 2001). These two methods were chosen because of their immense popularity and because in our experience they seem to work well in different regimes: XGBoost performs best in situations with low noise but complex mean functions, while random forests per-

forms best in situations with substantial noise (sources of unmeasured variation). A key finding of our simulations is that XBART performs well across this spectrum, making it a strong default choice when the quality of one’s data is unknown in advance. Additional comparisons with neural networks, using Keras (Chollet et al., 2015), are included in Appendix D along with implementation details. A good faith effort was made to cross-validate XGBoost and random forests thoroughly and efficiently, but additional improvements may be possible in the hands of a skilled user. All-the-same, a key practical advantage of XBART is a relatively automated model-fitting process. Although XBART itself has numerous tuning parameters — the number of trees, the number of sweeps, prior parameters, number of cutpoint candidates, and variable subsampling — all of the simulation results reported below are on a *single* set of parameters.

4.1 Simulation studies

The goal of these simulation studies is to examine the behavior of XBART regression across a variety of data generating processes (DGPs). Although no simulation study can be truly exhaustive, by varying several individual aspects of the data generating process, a performance profile emerges that suggests that XBART is a supervised learning algorithm of wide applicability. Specifically, function estimation at a set of hold-out locations was judged according to root mean squared error (RMSE).

All data generating processes are homoskedastic additive error models:

$$Y = f(\mathbf{x}) + \epsilon$$

with $E(\epsilon) = 0$. Within this framework many individual elements are varied: the mean function f , the error distribution, including its shape and its variance, the predictor variable matrix \mathbf{X} , specifically the number of individual features and the dependence between them, as well as the size of the training sample.

Mean functions

Four mean functions are considered, as defined in Table 1. The selection of these functions

was intended to cover a range of important special cases: linearity, additive models, models with interactions, nonlinear smooth functions, and functions with discontinuities. The value of using fixed functions as opposed to randomly generated polynomials, say, is that we can study coverage under repeated sampling. These functions were designed to be easily understandable to a human, but challenging to learn.

Name	Function
Linear	$\mathbf{x}^t \boldsymbol{\gamma}; \gamma_j = -2 + \frac{4(j-1)}{d-1}$
Single index	$10\sqrt{a} + \sin(5a); a = \sum_{j=1}^{10} (x_j - \gamma_j)^2; \gamma_j = -1.5 + \frac{j-1}{3}$.
Trig+poly	$5 \sin(3x_1) + 2x_2^2 + 3x_3x_4$
Max	$\max(x_1, x_2, x_3)$

Table 1: Four true f functions

Predictor variables

The $n \times p$ predictor matrix \mathbf{X} is generated in one of two ways:

1. Independent variables: each element of \mathbf{X} is drawn independently from a standard Gaussian distribution.
2. Correlated predictors with factor structure: row of \mathbf{X} is drawn from a Gaussian factor model with $k = p/5$ factors. Latent factor scores are drawn according to $\mathbf{F}_{k \times n} \sim N(0, 1)$. The factor loading matrix, $\mathbf{B}_{p \times k}$, has entries that are either zero or one, with exactly five ones in each column and a single 1 in each row, so that $\mathbf{B}\mathbf{B}^t$ is block diagonal, with blocks of all ones and all other elements being zero. The regressors are then set as $\mathbf{X} = (\mathbf{B}\mathbf{F})^T + \boldsymbol{\varepsilon}$ where $\boldsymbol{\varepsilon}$ is a $n \times p$ matrix of errors with independent $N(0, 0.01k)$ entries. Finally, each column of \mathbf{X} is scaled to standard deviation 1.

Error distribution

The error term ϵ is drawn in one of two ways:

1. Gaussian. Draw $\epsilon_i \stackrel{\text{iid}}{\sim} N(0, \sigma^2)$ and $\sigma^2 = \kappa^2 \text{Var}(f)$ where κ controls the signal-to-noise ratio.

$p = 30$	$p = 100$	$p = 500$	$p = 1,000$
$n = \begin{cases} 10,000, \\ 50,000, \\ 250,000 \end{cases}$	$n = 1,000$	$n = 300$	$n = \begin{cases} 500, \\ 1,000 \end{cases}$

Table 2: Sample sizes and number of predictors considered in the simulation study.

2. Student- t . Draw $\epsilon_i \stackrel{\text{iid}}{\sim} \kappa \sqrt{\text{Var}(f)} \times (t_3/\sqrt{3})$, a student- t distribution with degree of freedom 3. Note that the additional scaling factor $\sqrt{3}$ ensues variance of ϵ_i to be $\kappa^2 \text{Var}(f)$.

In each of these two cases, we consider $\kappa \in \{1, 10\}$.

Sample sizes and number of features (n and p)

Sample size and the number of features were considered in a variety of combinations and are reported in Table 2. Large and small sample sizes, including the case of more predictors than observations, are considered.

Hyper-parameter setting

The simulation studies use the default hyper-parameter settings as suggested in section 3.2.

4.1.1 Results

Complete simulation results are reported in tabular form in Appendix D. Here we summarize our findings, which are visualized in Figure 2. Figure 2 consists of six panels. The first column is the low noise setting, with $\kappa = 1$; the second column is the high noise setting, with $\kappa = 10$. The first two rows are for Gaussian errors with independent versus dependent predictors; the third row considers independent predictors with Student- t errors. Each point in the figure corresponds to a single realization (training and test set) from a particular data generating process, with sample sizes distinguished by character and true mean functions distinguished by color (see legend). In order to simultaneously compare three methods, the performance of random forests is used as a baseline, the horizontal and vertical axes represent the root mean square error of XBART and XGBoost, respectively,

as a proportion of the root mean square error of random forests. Thus, the regions of the plot have the following interpretations. Points above the dashed line at 1 indicate that XGBoost performed worse than random forests; points to the right of the vertical dashed line at 1 indicate that XBART performed worse than random forests; points above the diagonal indicate that XGBoost performed worse than XBART (irrespective of the performance of random forests). Accordingly: points in the upper right quadrant (defined by the dashed lines) are cases where random forests performed best; points in the lower triangle of the unit square (with lower left corner at the origin) are cases where XGBoost performed best; points in the upper triangle of the unit square are cases where XBART performed best. For each unique color and character combination there are five independent replications.

Several notable patterns emerge from these plots:

- More points lie above the dashed horizontal line in the right column compared to the left. This means: XGBoost performs better (relatively) in the low noise setting ($\kappa = 1$); random forests performs better (relatively) in the high noise setting ($\kappa = 10$).
- More points lie above the diagonal than below it, indicating that, overall, XBART performs better than XGBoost in both the low and high noise regimes.
- In the right column, points cluster along the vertical dashed line and the diagonal within the unit square. More specifically, in the large sample size cases (with symbols \times , ∇ , and \diamond), XBART and XGBoost have similar performance, while in the more challenging low sample cases XBART and random forests have similar performance, whereas XGBoost struggles (presumably due to inadequate regularization, despite cross-validation).
- Color-specific clusters emerge, especially in the left column. The linear function (black) clusters around the $(1, 1)$ point, indicating that all three methods perform similarly on this mean function. The max function (red) clusters just below the diagonal on the unit square, meaning that XGBoost performs slightly better than XBART, while random forest struggles.
- In a few high sample size cases, XBART struggles with the Student-t errors as indicated by the points in the lower right.

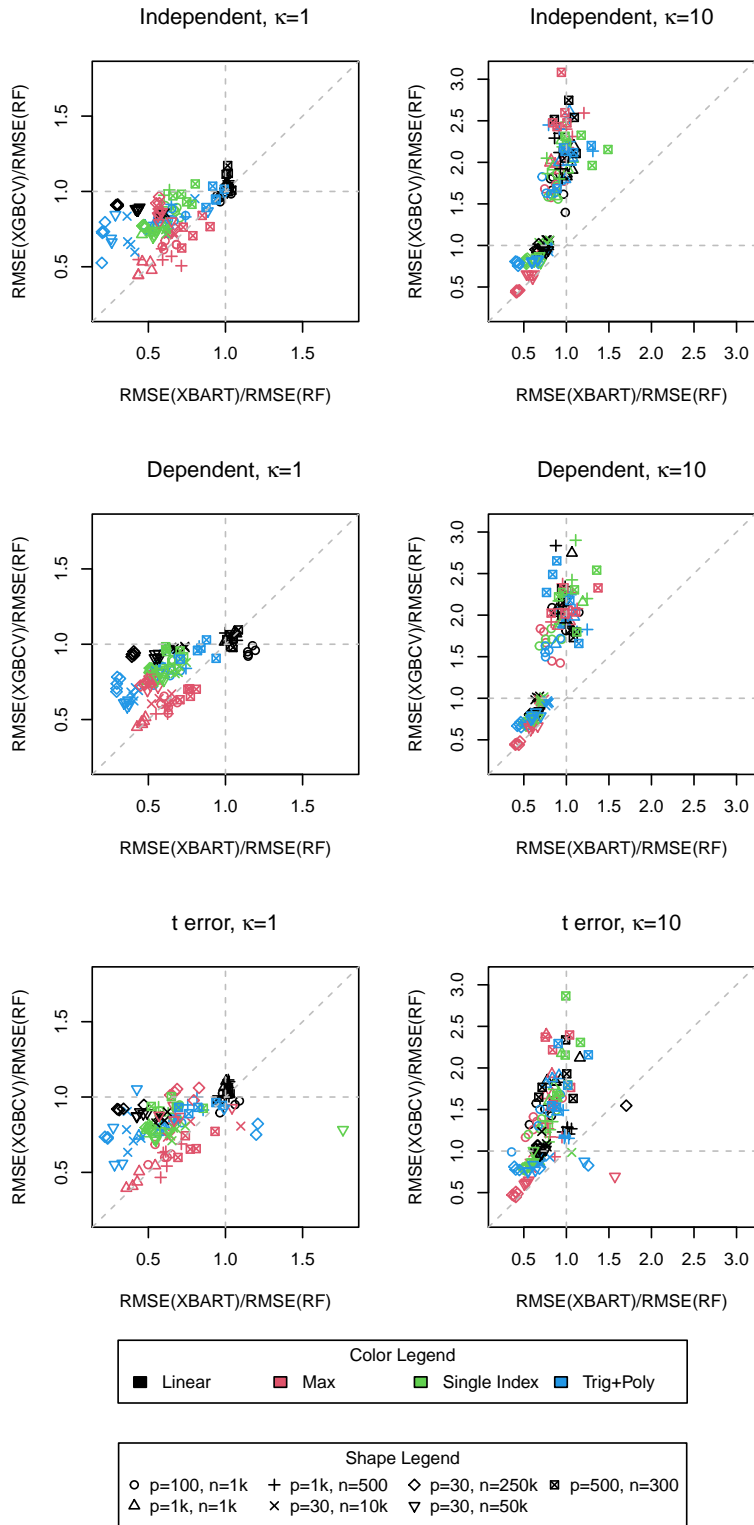


Figure 2: RMSE ratios of XBART to RF against XGBCV to RF across a variety of data generating processes.

Not depicted in the plot are running times, which can be found in the tables in Appendix D. The broad trend is simply this: XBART is as fast or faster, generally speaking, than cross-validated XGBoost and typically not more than twice as slow as random forests. With broadly comparable running speed and the favorable performance profile described above, XBART appears to be a strong default choice for nonlinear regression in a wide range of settings.

4.2 Out-of-sample prediction on empirical data

This section compares the predictive performance of XBART and alternative methods on seven different real data sets. These data sets are accessible at the UCI machine learning data repository (Dua and Graff, 2017). For each data set, 20 train-test splits are created by randomly drawing 5/6 of the data as training sets and the remaining 1/6 as testing sets. With 7 data sets a total of $7 \times 20 = 140$ random train-test splits were obtained.

XBART is run with default hyper-parameters as discussed in Section 3. The competitors are random forest and XGBoost both with and without cross-validation. The software packages and hyper-parameter settings are the same as were used in Section 4 and detailed in Appendix D.

To compare performance across different data sets, relative RMSE (RRMSE) is considered, which is the RMSE divided by the minimal RMSE for each data split: an RRMSE of 1.0 indicates that the method achieved the minimal RMSE on a given split. Figure 3 shows boxplots of RRMSE for each method across all data splits. Table 3 shows the average RMSE and running time (in seconds) of each method across the 20 random splits of each data set.

The upshot of Figure 3 is that XBART tends to outperform XGBoost, with or without cross-validation. Although random forest achieves smaller average RMSE, its performance varies significantly across different data set or data splits. Notably, cross-validated XGBoost has bigger RRMSE than the default XGBoost, which suggests overfitting the training data (and, moreover, suggests that the $\kappa = 10$ simulations are more analogous to these empirical data sets). Roughly speaking, it appears that XBART performs on par with random forests on weak-signal data sets where random forests excels and performs on par with XGBoost

Data name (source)	n	p	XBART	RF	XGBCV	XGB
CASP (Rana et al., 2015)	45730	9	3.89 (15.5)	3.49 (4.0)	3.74 (20.5)	4.15 (0.4)
Energy (Candanedo et al., 2017)	19735	29	77.63 (14.6)	68.27 (1.5)	74.61 (18.6)	80.01 (0.3)
AirQuality (De Vito et al., 2008)	9357	13	45.24 (2.2)	45.21 (0.5)	45.33 (6.1)	45.30 (0.1)
BiasCorrection (Cho et al., 2020)	7590	21	0.91 (2.3)	0.93 (0.5)	0.92 (5.1)	0.98 (0.1)
ElectricalStability (Arzamasov et al., 2018)	10000	14	0.0091 (10.0)	0.0130 (0.8)	0.0173 (13.8)	0.0105 (0.1)
GasTurbine (Kaya et al., 2019)	36733	9	0.0566 (11.3)	0.0529 (2.8)	0.0611 (13.6)	0.0617 (0.2)
ResidentialBuilding (Rafei and Adeli, 2016)	372	107	32.68 (0.9)	53.27 (0.1)	32.08 (6.8)	27.16 (0.1)

Table 3: Raw RMSE and running time (in parenthesis) of all methods on different real datasets. All measurements are average of 20 independent random splits of training / testing sets.

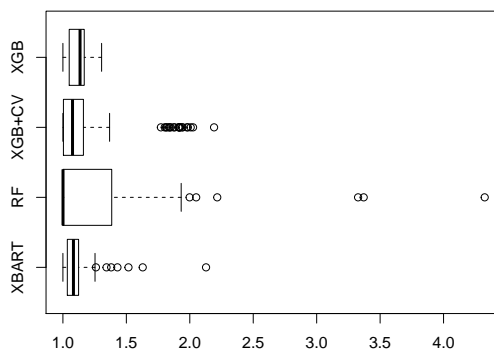


Figure 3: Boxplot of the RRMSE for each method across the total 120 training / testing splits.

on strong-signal data sets where XGBoost excels. This parallels the pattern observed in the simulation studies. Because in practice we often do not know which regime we are in, XBART appears to be a compelling default choice for nonlinear regression.

5 Warm-start BART MCMC

Standard BART MCMC (Chipman et al., 2010) initializes each tree at the root (i.e., a tree only one node) and explores the posterior over trees via a random-walk Metropolis-Hastings algorithm. This approach works surprisingly well in practice, but it is natural to wonder if it takes unnecessarily long to find favorable regions in tree space. Because XBART provides a fast approximation to the BART posterior, initializing BART MCMC at XBART trees

rather than roots is a promising strategy to help speed convergence and accelerate posterior exploration by running multiple chains. We find that this approach yields improved point estimation and posterior credible intervals with substantially higher pointwise frequentist coverage of the mean function and a fraction of the total run time.

Consider the data generating process described in section 4.1, with sample size $n = 10,000$ with varying noise levels κ . We fit 40 XBART sweeps, the first 15 are thrown out as burn-in draws, and 25 forest draws are retained. BART was fit with a burn-in of 1,000 samples, and 2,500 retrained posterior samples. For the warm-start BART, 25 *independent* BART MCMC chains were initialized at the 25 forest draws obtained from XBART, and each was run for 100 iterations without burn-in. Note that the total number of posterior draws is 2,500, the same as the number of posterior draws by BART. We repeat drawing synthetic data, and computing intervals 100 times. All measurements below were taken average with respect to those 100 replications.

		$\kappa = 1$			$\kappa = 2$		
DGP		XBART	BART	WS-BART	XBART	BART	WS-BART
Linear	coverage	0.78	0.77	0.99	0.50	0.83	0.98
	interval length	7.82	6.14	9.92	6.53	8.82	11.84
	running time	5.61	131.17	3.85 (101.86)	3.61	109.43	3.33 (86.86)
	RMSE	3.11	2.51	1.81	4.74	4.13	2.53
Max	coverage	0.86	0.78	0.95	0.88	0.84	0.97
	interval length	0.36	0.35	0.46	0.58	0.64	0.76
	running time	1.57	44.41	1.21 (31.82)	1.35	40.23	1.22 (31.85)
	RMSE	0.11	0.14	0.11	0.17	0.22	0.17
Single Index	coverage	0.77	0.73	0.87	0.81	0.83	0.91
	interval length	4.84	4.62	5.88	6.81	7.67	8.49
	running time	5.10	102.87	2.97 (79.35)	3.92	90.70	2.81 (74.05)
	RMSE	1.94	2.08	1.92	2.51	2.73	2.47
Trig+Poly	coverage	0.90	0.74	0.96	0.90	0.82	0.96
	interval length	3.61	2.89	4.23	5.62	5.06	6.86
	running time	4.68	92.75	3.02 (80.18)	3.68	86.81	2.90 (74.17)
	RMSE	1.03	1.27	1.01	1.65	1.87	1.60

Table 4: Coverage and length of credible interval of f at 95% level for warm-start BART (WS-BART) MCMC. The table also shows running time (in seconds) and root mean squared error (RMSE) of all approaches. The left panel is for noise level $\kappa = 1$ and the right panel is for higher noise level $\kappa = 2$.

Table 4 shows the credible interval coverage, length, RMSE of the point estimate, and running time of the three approaches. The running time for warm-start BART is reported as time in seconds for a single *independent* BART MCMC, while the number in parenthesis

is the running time of the entire warm-start BART fitting process, including the XBART fit and assuming all 25 independent warm-start BART MCMC were fitted *sequentially* rather than in parallel. In other words, the number in parentheses is the most conservative estimation of the total running time, because the 25 independent BART chains can be trivially parallelized to achieve much lower total running time. Indeed, with 25 processors, the run time would be the XBART run time plus the warm-start run time (not in parentheses).

Warm-start BART boasts a substantial advantage in terms of credible interval coverage and root mean squared error. In all cases, warm-start BART has the best coverage and RMSE among all three approaches and is still faster than BART under the most conservative running time estimation. When the true mean function is linear in x , warm-start initialization yields considerable improvement in the estimation, which may indicate inadequate chain length of BART (that is, poor mixing).

6 Preliminary theory

The XBART algorithm differs from BART or XGBoost. It is not a bagged estimator like random forests. It is not an optimization or stochastic optimization procedure, like CART or XGBoost. Neither is it a typical Markov chain Monte Carlo algorithm, like BART. Therefore, the usual frameworks for understanding supervised learning algorithms do not apply directly to XBART. On the one hand, the warm-start results in the previous section reassure us that XBART is a highly useful heuristic, even without a theoretical framework. On the other hand, an improved theoretical understanding would justify the use of XBART as a stand-alone algorithm and suggest avenues for future improvements and extensions. In this section, we prove two preliminary results about the XBART algorithm.

- First, we establish the theory that the single-tree version of the algorithm is asymptotically consistent. Here we rely critically on recent results for CART (and random forests) and adapt the proof strategy for XBART.
- Second, we prove that the forest (a sum of multiple trees) version of the algorithm defines a Markov chain that has a stationary distribution.

Taken together, these results suggest that the algorithm finds high-likelihood regions in parameter space and is not at risk of drifting aimlessly, which is consistent with the simulation evidence presented above.

6.1 Consistency

In this section, we establish the result that single-tree XBART regression is L^2 consistent. We do not consider variable subsampling and allow each tree to grow until reaching a max depth. As such, the results described in this section do not apply to the complete XBART algorithm, rather they help us to understand two key components of XBART that differentiate it from CART: stochastic sampling of the cutpoints and the use of BART’s marginal likelihood split criterion.

This section adapts the recent consistency results of CART and random forests (Scornet et al., 2015) to XBART with a single tree. More specifically, we show that the single-tree XBART satisfies the sufficient conditions stated in Scornet et al. (2015) for L^2 consistency. The proof in Scornet et al. (2015) proceeds by showing that the split criterion satisfies certain sufficient conditions, which are presented in the following section. To adapt this proof to XBART involves two steps. First, note that CART optimizes its split criterion to select a cutpoint, while XBART draws cutpoints at random. We reconcile this difference in the two methods — optimizing versus sampling of cutpoints — by applying the perturb-max lemma, showing the XBART’s cutpoint sampling strategy is equivalent to *optimizing* a random objective function, where the randomness vanishes asymptotically. Second, we prove that a key lemma used by Scornet et al. (2015) applies to the XBART split criterion as well.

We present the main result first. Theorem 1 states that a single-tree XBART fit approximates the true underlying mean function in the \mathcal{L}^2 norm if the maximum allowed depth goes to infinity slower than a certain function of the sample size. We state the theorem now in terms of a technical condition which will be defined shortly.

Theorem 1. *Assume Condition 1 (in the section of 6.1.3) holds and that $\|f\|_\infty < \infty$ and f is continuous on $[0, 1]^p$. Let $\hat{f}_n(\mathbf{x})$ denote a single-tree XBART fit (without variable subsampling and null cutpoint). Let $n \rightarrow \infty$, $d_n \rightarrow \infty$ and $(2^{d_n} - 1)(\log n)^9/n \rightarrow 0$. Then*

XBART is consistent in the sense that

$$\lim_{n \rightarrow \infty} \mathbb{E}[\widehat{f}_n(\mathbf{x}) - f(\mathbf{x})]^2 = 0,$$

where the expectation \mathbb{E} is over \mathbf{x} , which is uniformly distributed over $[0, 1]^p$.

Before proceeding, Section 6.1.1 reviews necessary notations. Then, Section 6.1.2 invokes the perturb-max theorem to show that the sampling cutpoint strategy of XBART is equivalent to optimizing a stochastic split criterion. Section 6.1.3 presents sufficient conditions (Condition 1 and Lemma 3) the split criterion must satisfy to guarantee tree consistency. The proof that Condition 1 and Lemma 3 imply Theorem 1 may be found in Scornet et al. (2015), which in turn appeals to Theorem 10.2 of Györfi et al. (2006).

6.1.1 Notation

Without loss of generality let $\mathbf{x} = (x_1, \dots, x_p)$ is uniformly distributed over $[0, 1]^p$ and $y \in \mathbb{R}$. The goal is to estimate the unknown mean function $f(\mathbf{x}) = \mathbb{E}[Y | \mathbf{x}]$ using data $\mathcal{D}_n = \{(y_1, \mathbf{x}_1), \dots, (y_n, \mathbf{x}_n)\}$. Denote the fitted XBART single tree by $\widehat{f}_n(\mathbf{x}; \mathcal{D}_n) : [0, 1]^p \rightarrow \mathbb{R}$. Let d_n denote maximum allowed depth of the tree. In the following sections, we will write $\widehat{f}_n(\mathbf{x})$ rather than $\widehat{f}_n(\mathbf{x}; \mathcal{D}_n)$ to lighten notation. As before, the $n \times p$ matrix $\mathbf{X} = (\mathbf{x}_1^t, \dots, \mathbf{x}_n^t)^t$ indicates all covariate data with n observations and p variables, and $\mathbf{x}_i = (x_i1, \dots, x_ip)$ is the covariate vector of the i -th observation.

6.1.2 Connection of XBART sampling to CART optimization

Both single-tree XBART and CART grow regression trees recursively, but use different procedures to select cutpoints: CART optimizes its split criterion while XBART draws cutpoints randomly with probability proportional to its (distinct) split criterion. However, these two cutpoint selection methods are not as different as they seem, due to a well-known result called the *perturb-max lemma*, which shows that random sampling is equivalent to optimizing an objective function. The perturb-max lemma shows XBART's drawing cutpoint strategy is equivalent to an optimization problem, thus made it possible to verify the sufficient conditions of consistency in Scornet et al. (2015), which is based on optimization,

is valid for XBART as well.

We restate this result (following the presentation in Hazan et al. (2016), Corollary 6.2) for reference.

Lemma 1 (Perturb-max, Hazan et al. (2016), Corollary 6.2). *Suppose there are $|\mathcal{C}|$ finite cutpoint candidates $\{c_{jk}\}$ at a specific node. Let $l(c_{jk}) = \log(L(c_{jk}))$ denote logarithm of the split criterion in expression (7). We are interested in drawing one of them according to probability $P(c_{jk}) = \frac{\exp[l(c_{jk})]}{\sum_{c_{jk} \in \mathcal{C}} \exp[l(c_{jk})]}$. We have*

$$\frac{\exp[l(c_{jk})]}{\sum_{c_{jk} \in \mathcal{C}} \exp[l(c_{jk})]} = P\left(c_{jk} = \arg \max_{c_{jk} \in \mathcal{C}} \{l(c_{jk}) + \gamma_{jk}\}\right) \quad (11)$$

where $\{\gamma_{jk}\}$ are independent random draws from a Gumbel(0,1) distribution with density $p(x) = \exp[-x + \exp(-x)]$.

Lemma 1 states that XBART sampling cutpoints according to the probability on the left-hand side of expression 11 can be achieved by the following steps:

1. Calculating $l(c_{jk})$ for all cutpoint candidates $c_{jk} \in \mathcal{C}$. Draw γ_{jk} from a Gumbel(0,1) distribution.
2. Pick cutpoint c_{jk} that maximizes the objective function $l(c_{jk}) + \gamma_{jk}$.

Next, note that this optimization problem is invariant if the objective function is scaled by a constant n , used here to denote the number of observations in the current node, so that

$$\arg \max_{c_{jk} \in \mathcal{C}} \frac{l(c_{jk})}{n} + \frac{\gamma_{jk}}{n},$$

and define the “empirical” split criterion as

$$L_n(c_{jk}) = \frac{l(c_{jk})}{n} + \frac{\gamma_{jk}}{n}. \quad (12)$$

Therefore, CART and single-tree XBART differ only in terms of the objective function (split criterion) they optimize. In the following proof of the main theorem, we verify that the empirical split criterion of XBART in equation (12) satisfies sufficient conditions for consistency.

Following the terminology of [Scornet et al. \(2015\)](#), we refer to the limit $L^*(c_{jk}) = \lim_{n \rightarrow \infty} L_n(c_{jk})$ as the “theoretical” split criterion, and $L_n(c_{jk})$ the “empirical” split criterion based on data with n observations. Furthermore, we refer to the tree growing by the empirical or the theoretical split criterion by “empirical tree”, and “theoretical tree” respectively.

Lemma 2. *Theoretical split criterion of XBART: By the strong law of large numbers, $L_n(c_{jk}) \rightarrow L^*(c_{jk})$ almost surely as $n \rightarrow \infty$, for all cutpoint c_{jk} , where*

$$L^*(c_{jk}) = \frac{1}{\sigma^2} \left[P(\mathbf{x}^{(j)} \leq c_{jk}) \left(\mathbb{E}(Y \mid \mathbf{x}^{(j)} \leq c_{jk}) \right)^2 + P(\mathbf{x}^{(j)} > c_{jk}) \left(\mathbb{E}(Y \mid \mathbf{x}^{(j)} > c_{jk}) \right)^2 \right]. \quad (13)$$

See the Appendix C for proof of the convergence.

Remark It is important for the proof to note that $L^*(c_{jk})$ does not rely on the training data. Observe also that the theoretical split criterion of XBART and CART are equivalent up to a linear transformation with constant coefficients².

6.1.3 Sufficient conditions of consistency

This section establishes sufficient conditions for a recursively fitting tree, with picking cut-point by optimization, to be L^2 consistent. The proof of the single-tree XBART algorithm satisfies those conditions are presented in the Supplementary Material.

The intuition behind the proof of consistency of CART in [Scornet et al. \(2015\)](#) is to show that variation of the true function over each hyper-rectangular cell (associated to a leaf node) shrinks as the number of data observations grows larger. Specifically, the variation within a cell can become small in one of two ways. Either, one, because the diameter (largest edge) of the cell shrinks to zero (and the function is continuous and has finite infinity norm). Or, two, because the true function is constant over any cell of non-shrinking diameter. This intuition can be formalized via two conditions.

Stating these conditions requires additional notation. To facilitate easy reference to [Scornet et al. \(2015\)](#), we follow their notations in this section. Write $c = (c^{(1)}, c^{(2)})$ to represent a cutpoint, where $c^{(1)} \in \{1, \dots, p\}$ indicates cut variables and $c^{(2)} \in [0, 1]$ indicates

²Specifically, the “theoretical” (asymptotic) CART and XBART criteria have the relationship $L_{\text{CART}}^*(c_{jk}) = [\mathbb{E}(Y \mid \mathbf{x} \in \mathcal{A})]^2 - \sigma^2 L_{\text{XBART}}^*(c_{jk})$, where \mathcal{A} is the current parent node, σ^2 is the error variance parameter within the XBART model, which is assumed fixed, but need not equal the true error variance. See the supplementary material for a proof.

cut values. A sequence of k cutpoints from the root until depth k is $\mathbf{c}_k = (c_1, \dots, c_k)$, where $c_k = (c_k^{(1)}, c_k^{(2)})$ is the k -th cutpoint. Let $\mathcal{A}_n(\mathbf{x}, \mathbf{\Gamma})$ denote the leaf node of an *empirical tree* (growing by the empirical split criterion) built with random parameter $\mathbf{\Gamma}$ that contains \mathbf{x} . Let $\mathcal{A}_k^*(\mathbf{x}, \mathbf{\Gamma})$ be a cell of the *theoretical tree* (growing by the theoretical split criterion) at depth k containing \mathbf{x} . Additionally, $\mathcal{A}(\mathbf{x}, \mathbf{c}_k)$ is the node containing \mathbf{x} in the tree built with the sequence of cutpoints \mathbf{c}_k , and we call $\mathbb{A}_k(\mathbf{x})$ the set of all possible $k \geq 1$ cutpoints used to create the node containing \mathbf{x} . The distance between two cut sequences $\mathbf{c}_k, \mathbf{c}'_k \in \mathbb{A}_k(\mathbf{x})$ is defined as

$$\|\mathbf{c}_k - \mathbf{c}'_k\|_\infty = \sup_{1 \leq j \leq k} \max\left(\left|c_j^{(1)} - c'_j{}^{(1)}\right|, \left|c_j^{(2)} - c'_j{}^{(2)}\right|\right).$$

The distance between a cut \mathbf{c}_k and a set $\mathbb{A} \subset \mathbb{A}_k(\mathbf{x})$ is defined as

$$c_\infty(\mathbf{c}_k, \mathbb{A}) = \inf_{\mathbf{c} \in \mathbb{A}} \|\mathbf{c}_k - \mathbf{c}\|_\infty.$$

Define the total variation of f within any leaf node \mathcal{A} as

$$\Delta(f, \mathcal{A}) = \sup_{\mathbf{x}, \mathbf{x}' \in \mathcal{A}} |f(\mathbf{x}) - f(\mathbf{x}')|.$$

We may now state the first condition invoked in Theorem 1³.

Condition 1 (Vanishing total variation). *For all $x \in (0, 1)^p$,*

$$\Delta(f, \mathcal{A}_k^*(\mathbf{x}, \mathbf{\Gamma})) \rightarrow 0 \quad \text{almost surely as } k \rightarrow \infty.$$

Condition 1 states that as $n \rightarrow \infty$, variation of the true function f tends to zero in the leaf nodes of a *theoretical tree*. [Scornet et al. \(2015\)](#) show that Condition 1 is satisfied by CART if f is additive, the elements of \mathbf{x} are independent, and the errors are Gaussian (their Lemma 1 and assumption 1). Because XBART and CART have the same theoretical split criterion (see the supplementary material for a proof), their proof applies directly to XBART, so Condition 1 is satisfied for us as well if f satisfies those rather strict requirements. Plausibly, Condition 1 is satisfied for a broader class of functions in

³The Condition 1 and Lemma 1 in this paper correspond to Lemma 1 and Lemma 2 in [Scornet et al. \(2015\)](#) respectively.

conjunction with the XBART (equivalently, CART) theoretical tree and for this reason we feel that Condition 1 is better treated as an assumption.

Now we move on to Lemma 3, which states that the cutpoints of the theoretical and empirical trees are close to one other in a certain sense. For any $\mathbf{x} \in [0, 1]^p$, and cuts \mathbf{c}_k , define the empirical split criterion (as of equation (12)) for XBART as

$$\begin{aligned}
L_{n,k}(\mathbf{x}, \mathbf{c}_k) &= \frac{\tau N_n(\mathcal{A}_L)}{\sigma^2(\sigma^2 + \tau N_n(\mathcal{A}_L))} \frac{1}{n} \left(\sum_{i: x_i^{(c_k^{(1)})} \leq c_k^{(2)}} y_i^2 - \sum_{i: x_i^{(c_k^{(1)})} \leq c_k^{(2)}} (y_i - \bar{y}_l)^2 \right) \\
&+ \frac{\tau N_n(\mathcal{A}_R)}{\sigma^2(\sigma^2 + \tau N_n(\mathcal{A}_R))} \frac{1}{n} \left(\sum_{i: x_i^{(c_k^{(1)})} > c_k^{(2)}} y_i^2 - \sum_{i: x_i^{(c_k^{(1)})} > c_k^{(2)}} (y_i - \bar{y}_r)^2 \right) \\
&+ \frac{\gamma_{\mathbf{x}}}{n}.
\end{aligned} \tag{14}$$

where $N_n(\mathcal{A}_L)$ and $N_n(\mathcal{A}_R)$ are number of data observations in the node $\mathcal{A}(\mathbf{x}, \mathbf{c}_{k-1}) \cap \{\mathbf{z} : z^{(c_k^{(1)})} \leq c_k^{(2)}\}$ and $\mathcal{A}(\mathbf{x}, \mathbf{c}_{k-1}) \cap \{\mathbf{z} : z^{(c_k^{(1)})} > c_k^{(2)}\}$ respectively and \bar{y}_l and \bar{y}_r denote the left and right observation means. The function $L_{n,k}(\mathbf{x}, \mathbf{c}_k)$ is the empirical split criterion for the node $\mathcal{A}(\mathbf{x}, \mathbf{c}_{k-1})$ expressed in terms of previous cuts \mathbf{c}_{k-1} and the current cut c_k . For all $\xi > 0$ and $\mathbf{x} \in [0, 1]^p$, $\mathbb{A}_{k-1}^\xi(\mathbf{x}) \subset \mathbb{A}_{k-1}(\mathbf{x})$ denotes the set of all sequences of cuts \mathbf{c}_{k-1} such that the node $\mathcal{A}(\mathbf{x}, \mathbf{c}_{k-1})$ contains a hypercube with edge length ξ . The set $\bar{\mathbb{A}}_k^\xi(\mathbf{x}) = \{\mathbf{c}_k : \mathbf{c}_{k-1} \in \mathbb{A}_{k-1}^\xi(\mathbf{x})\}$ is equipped with norm $\|\cdot\|_\infty$. We may now state the key lemma required in Scornet et al. (2015) to prove Theorem 1.

Lemma 3 (Stochastic equicontinuity). *Assume that $\|f\|_\infty < \infty$ and f is continuous on $[0, 1]^p$. Fix $\mathbf{x} \in [0, 1]^p$, $k \in \mathbb{N}^*$ and let $\xi > 0$. Then $L_{n,k}(\mathbf{x}, \cdot)$ is stochastically equicontinuous on $\bar{\mathbb{A}}_k^\xi(\mathbf{x})$: for all $\alpha, \rho > 0$, there exist $\delta > 0$ such that*

$$\lim_{n \rightarrow \infty} \mathbb{P} \left[\sup_{\substack{\|\mathbf{c}_k - \mathbf{c}'_k\|_\infty \leq \delta \\ \mathbf{c}_k, \mathbf{c}'_k \in \bar{\mathbb{A}}_k^\xi(\mathbf{x})}} |L_{n,k}(\mathbf{x}, \mathbf{c}_k) - L_{n,k}(\mathbf{x}, \mathbf{c}'_k)| > \alpha \right] \leq \rho.$$

A proof that Lemma 3 holds for XBART split criterion in equation (14) is presented in the Supplementary Material. Our proof strategy is the same as Scornet et al. (2015), but had to be verified using new bounding arguments specific to the XBART criterion.

6.2 Stationarity of the forest algorithm

This section proves that a slightly modified version of GROWFROMROOT generates draws from a Markov chain with a stationary distribution. The slight modification is that all leaf parameters are drawn jointly, conditional on the current state of the forest, prior to sampling (growing) each new tree.

Theorem 2. *XBART samples $\mathcal{F} = \{T_h\}_{1 \leq h \leq L}$ according to a finite-state Markov chain with stationary distribution.*

Proof. The proof proceeds by showing that the forest sampling process 1) is a Markov chain, 2) has only finite states, and 3) that the transition probability between any two states is positive. Therefore, by standard results (for example Theorem 1.7 and 1.20 of [Durrett \(2016\)](#)), it possesses a stationary distribution.

Let $\mathcal{F} = \{T_h\}_{1 \leq h \leq L}$ denote the forest of L trees and let $\boldsymbol{\mu} = \{\boldsymbol{\mu}_h\}_{1 \leq h \leq L}$ denote the associated leaf parameters. Let $\mathcal{F}_{-j} = \{T_h\}_{1 \leq h \leq L}/T_j$ and $\boldsymbol{\mu}_{-j} = \{\boldsymbol{\mu}_h\}_{1 \leq h \leq L}/\boldsymbol{\mu}_j$ be sets of trees and leaf parameters excepting the j th one.

1. GROWFROMROOT explicitly updates T_j given \mathcal{F}_{-j} and therefore defines a Markov chain. More explicitly, $\mathcal{F}^{(k)}$ is drawn by sampling and replacing tree T_j , conditional on $\mathcal{F}_{-j}^{(k-1)}$.
2. GROWFROMROOT samples trees from a finite state space. Each tree has a maximum depth and all cutpoint candidates are defined in terms of a finite predictor matrix \mathbf{X} , so the total number of tree configurations is finite. The forest \mathcal{F} is an ensemble of a finite number of trees, thus has a finite number of states as well.
3. The probability that GROWFROMROOT draws a given tree is a product of the non-zero probabilities of drawing specific cutpoints at each node; therefore, the probability of drawing any specific tree is non-zero.

Specifically,

$$p\left(T_j^{(k)} \mid \mathcal{F}^{(k-1)}\right) = \int p\left(T_j^{(k)} \mid y, \mathcal{F}_{-j}^{(k-1)}, \boldsymbol{\mu}_{-j}\right) \pi\left(\boldsymbol{\mu}_{-j}, \sigma^2 \mid y, \mathcal{F}^{(k-1)}\right) d\left(\boldsymbol{\mu}_{-j}, \sigma^2\right) > 0, \quad (15)$$

for any T_j . The second factor of the integrand, $\pi(\boldsymbol{\mu}_{-j}, \sigma^2 \mid y, \mathcal{F}^{(k-1)})$, denotes a draw from a conjugate linear regression with design matrix given by dummy variables indicating leaf membership (and simply discarding the parameters associated with the j th tree). The first factor in the integrand, $p(T_j^{(k)} \mid y, \mathcal{F}_{-j}^{(k-1)}, \boldsymbol{\mu}_{-j})$ denotes the product of GROWFROMROOT probabilities leading to a draw of T_j . Both factors are always greater than zero.

Finally, observe that there is at least one way to transition from any forest \mathcal{F} to any other forest \mathcal{F}' , which is to regrow each tree and replace them one by one over exactly L iterations.

□

7 Discussion

To conclude, we briefly describe the chronological development of the XBART algorithm, to provide additional context for evaluating the relative merits of XBART, BART (fit with traditional MCMC), and XGBoost.

The XBART algorithm grew out of our attempts to better understand BART’s exceptional empirical performance. In routine use, we found that BART often outperformed XGBoost at function estimation and prediction, sometimes substantially so. Unfortunately, there were some data sets that were simply too large for us to apply BART to, while XGBoost is notoriously fast. Our initial hypothesis was that BART’s clever regularization might be behind its remarkable performance, so we set about to create a fast recursive tree-fitting algorithm that utilized a penalty analogous to the BART prior. We found that this approach did not work as well as BART. Next, we conjectured that the BART splitting criterion might itself be the source of BART’s advantage and we implemented a version that greedily optimized BART’s marginal likelihood criteria when growing the trees. This too, did not match BART’s performance, so we decided to try sampling the cutpoints as currently performed in XBART, while optimizing the leaf parameters (rather than sampling). This led to a notable improvement, but still typically under-performed BART in our comparisons. So, we implemented the sampling of the leaf parameters, leading to the XBART

algorithm described in this paper. In addition, we notice that sampling the prior variance τ improves the performance on high noise and few data observations cases significantly. Finally, at this point, our new algorithm mimicked BART’s performance and sometimes even outperformed it — especially in larger problems where BART could not be run long enough to achieve adequate mixing.

To put this journey into perspective, our initial goal was to create a CART-like recursive optimization algorithm and introduce certain elements of BART. But, one by one as we incorporated these elements, each one yielded additional performance gains. In the end, we ended up with a BART fitting algorithm with a novel recursive growing scheme — mostly BART with a dash of CART, rather than vice-versa as we had initially planned.

The end result of these experiments and the accompanying algorithm development was the completely novel function estimation method described in Section 3. The remainder of the paper represents our attempts to better understand the operating characteristics of the new algorithm. Our key findings were that it has excellent performance on simulated and empirical data across various signal-to-noise regimes and test functions (Section 4). We also confirmed that it provides superior estimation and inference when used to initialize the BART MCMC algorithm, compared to the standard initialization scheme (Section 5). Finally, we were able to establish several basic theoretical facts about the algorithm (Section 6). Though these theoretical results are limited, they also address many of the primary objections one might have regarding a pseudo-Bayesian sampling algorithm, namely consistency and stationarity. Extending the single-tree results presented here to the ensemble version of the model is the subject of ongoing research.

BART has proven to be a widely used model in many fields, combining state-of-the-art estimation and prediction with fully Bayesian uncertainty quantification. The XBART algorithm permits these virtues to be realized on large data sets that were previously out of reach for existing implementations. The generality of the GROWFROMROOT algorithm suggests that the recursive stochastic search strategy at the heart of XBART can be readily adapted to other models and could yield similar accuracy and computational efficiency improvements as those seen in regression problems.

References

- Arzamasov, V., K. Böhm, and P. Jochem (2018). Towards concise models of grid stability. In *2018 IEEE International Conference on Communications, Control, and Computing Technologies for Smart Grids (SmartGridComm)*, pp. 1–6. IEEE.
- Bekkerma, R. (2015). The present and the future of the kdd cup competition: an outsider’s perspective.
- Breiman, L. (2001). Random forests. *Machine learning* 45(1), 5–32.
- Breiman, L., J. Friedman, R. Olshen, and C. J. Stone (1984). *Classification and regression trees*. Chapman and Hall/CRC.
- Brownlee, J. (2016). A gentle introduction to xgboost for applied machine learning.
- Candanedo, L. M., V. Feldheim, and D. Deramaix (2017). Data driven prediction models of energy use of appliances in a low-energy house. *Energy and buildings* 140, 81–97.
- Chen, T. and C. Guestrin (2016). XGBoost: A scalable tree boosting system. In *Proceedings of the 22nd ACM SIGKDD International Conference on Knowledge Discovery and Data Mining*, pp. 785–794. ACM.
- Chipman, H. A., E. I. George, R. E. McCulloch, et al. (2010). BART: Bayesian additive regression trees. *The Annals of Applied Statistics* 4(1), 266–298.
- Cho, D., C. Yoo, J. Im, and D.-H. Cha (2020). Comparative assessment of various machine learning-based bias correction methods for numerical weather prediction model forecasts of extreme air temperatures in urban areas. *Earth and Space Science* 7(4), e2019EA000740.
- Chollet, F. et al. (2015). Keras.
- De Vito, S., E. Massera, M. Piga, L. Martinotto, and G. Di Francia (2008). On field calibration of an electronic nose for benzene estimation in an urban pollution monitoring scenario. *Sensors and Actuators B: Chemical* 129(2), 750–757.

- Dua, D. and C. Graff (2017). UCI machine learning repository.
- Durrett, R. (2016). *Essentials of stochastic processes*, Volume 1. Springer.
- Friedman, J. H. (2001). Greedy function approximation: a gradient boosting machine. *Annals of Statistics*, 1189–1232.
- Friedman, J. H. (2002). Stochastic gradient boosting. *Computational Statistics & Data Analysis* 38(4), 367–378.
- Györfi, L., M. Kohler, A. Krzyzak, and H. Walk (2006). *A distribution-free theory of nonparametric regression*. Springer Science & Business Media.
- Hastie, T., R. Tibshirani, J. Friedman, and J. Franklin (2005). The elements of statistical learning: data mining, inference and prediction. *The Mathematical Intelligencer* 27(2), 83–85.
- Hazan, T., G. Papandreou, and D. Tarlow (2016). *Perturbations, Optimization, and Statistics*. MIT Press.
- He, J., S. Yalov, and P. R. Hahn (2019). XBART: Accelerated Bayesian additive regression trees. In *The 22nd International Conference on Artificial Intelligence and Statistics*, pp. 1130–1138.
- Hill, J., A. Linero, and J. Murray (2020). Bayesian additive regression trees: A review and look forward. *Annual Review of Statistics and Its Application* 7.
- Kaya, H., P. TÜFEKÇİ, and E. Uzun (2019). Predicting co and no x emissions from gas turbines: novel data and a benchmark pems. *Turkish Journal of Electrical Engineering & Computer Sciences* 27(6), 4783–4796.
- Ke, G., Q. Meng, T. Finley, T. Wang, W. Chen, W. Ma, Q. Ye, and T.-Y. Liu (2017). LightGBM: A highly efficient gradient boosting decision tree. In *Advances in Neural Information Processing Systems*, pp. 3146–3154.
- Laurent, B. and P. Massart (2000). Adaptive estimation of a quadratic functional by model selection. *Annals of Statistics*, 1302–1338.

- Lei, J., M. G'Sell, A. Rinaldo, R. J. Tibshirani, and L. Wasserman (2018). Distribution-free predictive inference for regression. *Journal of the American Statistical Association* 113(523), 1094–1111.
- Linero, A. R. (2017). A review of tree-based Bayesian methods. *Communications for Statistical Applications and Methods* 24(6).
- Linero, A. R. (2018). Bayesian regression trees for high-dimensional prediction and variable selection. *Journal of the American Statistical Association* 113(522), 626–636.
- Mehta, M., R. Agrawal, and J. Rissanen (1996). SLIQ: A fast scalable classifier for data mining. In *International Conference on Extending Database Technology*, pp. 18–32. Springer.
- Pafka, S. (2015). Benchmarking random forest implementations.
- Rafiei, M. H. and H. Adeli (2016). A novel machine learning model for estimation of sale prices of real estate units. *Journal of Construction Engineering and Management* 142(2), 04015066.
- Rana, P. S., H. Sharma, M. Bhattacharya, and A. Shukla (2015). Quality assessment of modeled protein structure using physicochemical properties. *Journal of bioinformatics and computational biology* 13(02), 1550005.
- Scornet, E., G. Biau, J.-P. Vert, et al. (2015). Consistency of random forests. *The Annals of Statistics* 43(4), 1716–1741.
- Wright, M. N. and A. Ziegler (2015). ranger: A fast implementation of random forests for high dimensional data in C++ and R. *arXiv preprint arXiv:1508.04409*.

A Computational considerations

This section catalogs implementation details that improve the computational efficiency of the algorithm. These implementational details serve to make the algorithm competitive with state-of-the-art supervised learning algorithms, such as XGBoost. These particular strategies, such as variable presorting and careful handling of categorical covariates, are inapplicable in the standard BART MCMC and XBART’s ability to incorporate them is the basis of its improved performance.

A.1 Adaptive variable importance weights

Our XBART implementation strikes an intermediate balance between the local BART updates, which randomly consider one variable at a time, and the all-variables Bayes rule described above. Specifically, we consider only $m \leq V$ variables at a time when sampling each cutpoint. Rather than drawing these variables uniformly at random as is done in random forests, we introduce a parameter vector w , which denotes the prior probability that a given variable is chosen to be split on, as suggested in [Linero \(2018\)](#). Before sampling each cutpoint, we randomly select m variables (without replacement) with probability proportional to w .

A.2 Pre-sorting predictor variables

Observe that the XBART split criterion depends on sufficient statistics only, namely the sum of the observations in a node (that is, at a given level of the recursion). An important implication of this, for computation, is that with sorted predictor variables, the various cutpoint integrated likelihoods can be computed rapidly via a single sweep through the data (per variable), taking cumulative sums. Let \mathbf{O} denote the V -by- n array such that o_{vh} denotes the index, in the data, of the observation with the h -th smallest value of the v -th predictor variable x_v . Then, taking the cumulative sums gives

$$s(\leq, v, c) = \sum_{h \leq c} r_{o_{vh}}$$

and

$$s(>, v, c) = \sum_{h=1}^n r_{lh} - s(\leq, v, c).$$

The subscript l on the residual indicates that these evaluations pertain to the update of the l -th tree.

The above formulation is useful if the data can be presorted and, furthermore, the sorting can be maintained at all levels of the recursive tree-growing process. To achieve this, we must loop over (sift) each of the variables before passing to the next level of the recursion. Specifically, we form two new index matrices \mathbf{O}^{\leq} and $\mathbf{O}^{>}$ that partition the data according to the selected cutpoint. For the selected split variable v and selected split c , this is automatic: $O_v^{\leq} = O_{v,1:c}$ and $O_v^{>} = O_{v,(c+1):n}$. For the other $V - 1$ variables, we sift them by looping through all n available observations, populating O_q^{\leq} and $O_q^{>}$, for $q \neq v$, sequentially, with values o_{qj} according to whether $x_{vo_{qj}} \leq c$ or $x_{vo_{qj}} > c$, for $j = 1, \dots, n$.

Because the data is processed in sorted order, the ordering will be preserved in each of the new matrices \mathbf{O}^{\leq} and $\mathbf{O}^{>}$. This strategy was first presented in [Mehta et al. \(1996\)](#) in the context of classification algorithms and has been rediscovered a number of times since then. The pre-sorting and sifting \mathbf{O} strategy is easy to implement for continuous covariates, but not for categorical covariates due to the possibility of ties in the data. [Appendix A.5](#) describes a special data structure for dealing with ties efficiently.

A.3 Adaptive cutpoint grid

Evaluating the integrated likelihood criterion is straightforward, but the summation and normalization required to sample the cutpoints contribute a substantial computational burden itself. Therefore, it is helpful to consider a restricted number of cutpoints C .

This can be achieved simply by taking every j th value (starting from the smallest) as an eligible cutpoint with $j = \lfloor \frac{n_b - 2}{C} \rfloor$. As the tree grows deeper, the amount of data that is skipped over diminishes. Eventually, we get $n_b < C$, and each data point defines a unique cutpoint. In this way, the data could, without regularization, be fit perfectly, even though the number of cutpoints at any given level is given an upper limit. As a default, we set the number of cutpoints to $\min(n, 100)$, where n is the sample size of the entire data set.

Our cutpoint subsampling strategy is more straightforward than the elaborate cutpoint subselection search heuristics used by XGBoost (Chen and Guestrin, 2016) and LightGBM (Ke et al., 2017), which both consider the gradient evaluated at each cutpoint when determining the next split. Our approach does not consider the response information at all but rather defines a predictor-dependent prior on the response surface. That is, given a design matrix \mathbf{X} , sample functions can be drawn from the prior distribution by sampling trees, splitting uniformly at random among the cutpoints defined by the node-specific quantiles, in a sequential fashion.

A.4 Variable importance weights

XBART can strike a balance between local BART updates, which randomly consider one variable at a time, and the all-variables Bayes rule described above by only considering $m \leq V$ variables when evaluating the cutpoints. Rather than drawing these m variables uniformly at random, as is done in random forests, we introduce a parameter vector w , which denotes the prior probability that a given variable is chosen to be split on, as suggested in Linero (2018). Before sampling each cutpoint, we randomly select m variables (without replacement) with probability proportional to w .

The variable weight parameter w is given a Dirichlet prior with hyper-parameters \bar{w} that is initialized to all ones. At each iteration of the first sweep through the forest, \bar{w} is incremented to count the total number of splits across all trees. The split counts are then updated in between each tree sampling/growth step:

$$\bar{w} \leftarrow \bar{w} - \bar{w}_l^{(k-1)} + \bar{w}_l^{(k)}$$

where $\bar{w}_l^{(k)}$ denotes the length- V vector recording the number of splits on each variable in tree l at iteration k . The weight parameter is then re-sampled as $w \sim \text{Dirichlet}(\bar{w})$. Splits that improve the likelihood function will be chosen more often than those that do not. The parameter w is then updated to reflect that, making chosen variables more likely to be considered in subsequent sweeps. In practice, we find it is helpful to use all V variables during an initialization phase, to more rapidly obtain an accurate initial estimate of w .

A.5 Categorical covariates

Section A.2 suggests pre-sorting covariates to compute sufficient statistics efficiently, this strategy is straightforward for continuous covariates. However, because of possible ties in ordered categorical covariates, a more efficient algorithm is needed to calculate sufficient statistics.

We restate notations in section A.2. Without loss of generality, we assume that all covariates are categorical. Let \mathbf{O} denote the V -by- n array such that o_{vh} denotes the index, in the data, of the observation with the h -th smallest value of the v -th predictor variable x_v . Then, taking the cumulative sums gives

$$s(\leq, v, c) = \sum_{h \leq c} r_{o_{vh}}$$

and

$$s(>, v, c) = \sum_{h=1}^n r_{lh} - s(\leq, v, c).$$

Algorithm 4 Pseudocode of calculating sufficient statistics for categorical covariates.

- 1: Sort categorical covariates, create \mathbf{O} matrix. Count number of unique observations `unique_val` and `val_count` vector (suppose vectors are length K).
- 2: **for** i from 1 to K **do**
- 3: Calculate sufficient statistics for cutpoint candidate `unique_val[i]` as

$$s(\leq, v, \text{unique_val}[i]) = \sum_{h \in [\sum_{m=1}^{i-1} \text{val_count}[m], \sum_{m=1}^i \text{val_count}[m]]} r_{o_{vh}}.$$

and

$$s(>, v, c) = \sum_{h=1}^n r_{lh} - s(\leq, v, c).$$

- 4: **end for**
 - 5: Calculate split criterion, determine a cutpoint.
 - 6: **if** stop-splitting is selected or stop conditions are reached **then**
 - 7: Draw leaf parameters and **return**.
 - 8: **else**
 - 9: Sift `unique_val` and `val_count` for left and right child nodes. Repeat step 3 when evaluate split criterion at child nodes.
 - 10: **end if**
-

The subscript l on the residual indicates that these evaluations pertain to the update of

the l th tree. Notice that when covariates are categorical, x_{vh} is not necessarily smaller than $x_{v(h+1)}$ due to potential ties in x . As a result, the number of unique cutpoint candidates is less than n . We propose an extra data structure to bookkeeping unique cutpoint and number of ties as follows. For the v -th categorical predictor variable x_v , let `unique_val` be a vector of unique values (sorted, from small to large) in x_v and `val_count` be a vector of counts of replication for each unique value. Therefore, the cutpoint candidate is a element in the vector `unique_val`, say the i -th element. Then the cumulative sums is

$$s(\leq, v, \text{unique_val}[i]) = \sum_{h \in [\sum_{m=1}^{i-1} \text{val_count}[m], \sum_{m=1}^i \text{val_count}[m]]} r_{o_{vh}}.$$

When sifting data to left and right child after drawing a cutpoint, we create the same `unique_val` and `val_count` vector for all categorical covariates with data in two child nodes respectively. See Algorithm 4 for details.

B Demo of XBART algorithm

Figure 4 depicts the fitting process of a simple XBART forest with three trees and two sweeps. We label the fitting target of each tree in each sweep explicitly.

C Convergence of the empirical split criterion (Lemma 2)

We show that the empirical split criterion in equation (12) converges to the theoretical one (13). Note that γ_{jk} is a draw from Gumbel(0,1) distribution.

$$\begin{aligned} L_n(c_{jk}) &= \frac{l(c_{jk})}{n} + \frac{\gamma_{jk}}{n} \\ &= \frac{1}{n} \frac{\tau n_{jk}^l}{\sigma^2 (\sigma^2 + \tau n_{jk}^l)} \left(\sum_{i: x_i \in \mathcal{A}_L(j,k)} y_i^2 - \sum_{i: x_i \in \mathcal{A}_L(j,k)} (y_i - \bar{y}_l)^2 \right) \\ &\quad + \frac{1}{n} \frac{\tau n_{jk}^r}{\sigma^2 (\sigma^2 + \tau n_{jk}^r)} \left(\sum_{i: x_i \in \mathcal{A}_R(j,k)} y_i^2 - \sum_{i: x_i \in \mathcal{A}_R(j,k)} (y_i - \bar{y}_r)^2 \right) \\ &\quad + \frac{1}{n} \log \left(\frac{\sigma^2}{\sigma^2 + \tau n_{jk}^l} \right) + \frac{1}{n} \log \left(\frac{\sigma^2}{\sigma^2 + \tau n_{jk}^r} \right) + \frac{1}{n} \gamma_{jk}. \end{aligned} \tag{16}$$

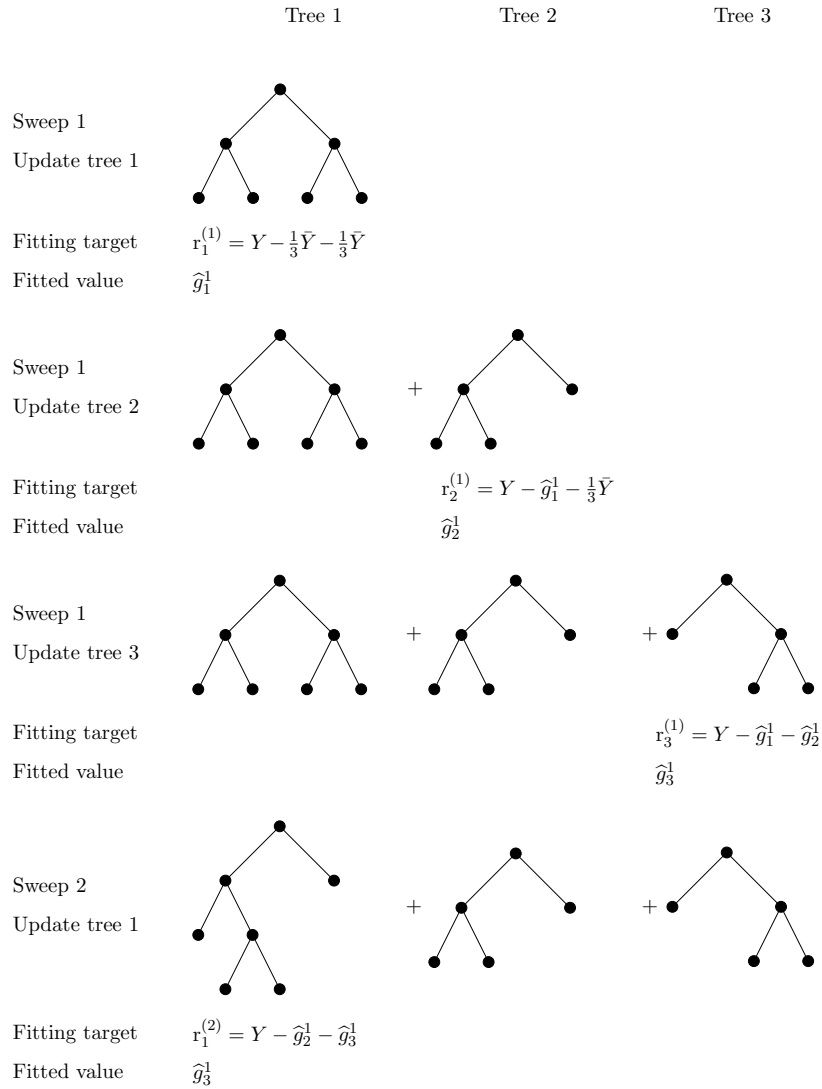


Figure 4: A simple demonstration of the XBART forest fitting procedure, where \bar{Y} denote average of all Y observations. It shows how to initialize the fitted values for the three trees in the first sweep, and update the first tree in sweep 2. The following sweeps update similarly.

As $n \rightarrow \infty$, since $n_{jk}^l < n$, it is straight forward that the last three terms converge to zero,

$$\frac{1}{n} \log \left(\frac{\sigma^2}{\sigma^2 + \tau n_{jk}^l} \right) \rightarrow 0, \quad \frac{1}{n} \log \left(\frac{\sigma^2}{\sigma^2 + \tau n_{jk}^r} \right) \rightarrow 0, \quad \frac{1}{n} \gamma_{jk} \rightarrow 0.$$

Furthermore, notice that $\frac{n_{jk}^l}{n}$ converges to $P(\mathbf{x}^{(j)} \leq c_{jk})$, the probability that a new observation falls in the left child, and similarly for $\frac{n_{jk}^r}{n}$. The first term of equation (16) converges to

$$\begin{aligned} & \frac{1}{n} \frac{\tau n_{jk}^l}{\sigma^2 (\sigma^2 + \tau n_{jk}^l)} \left(\sum_{i: \mathbf{x}_i \in \mathcal{A}_L(j,k)} y_i^2 - \sum_{i: \mathbf{x}_i \in \mathcal{A}_L(j,k)} (y_i - \bar{y}_l)^2 \right) \\ &= \frac{\tau n_{jk}^l}{\sigma^2 (\sigma^2 + \tau n_{jk}^l)} \frac{n_{jk}^l}{n} \left(\frac{1}{n_{jk}^l} \sum_{i: \mathbf{x}_i \in \mathcal{A}_L(j,k)} y_i^2 - \frac{1}{n_{jk}^l} \sum_{i: \mathbf{x}_i \in \mathcal{A}_L(j,k)} (y_i - \bar{y}_l)^2 \right) \\ &\rightarrow \frac{1}{\sigma^2} P(\mathbf{x}^{(j)} \leq c_{jk}) \left[\mathbb{E}(y^2 \mid \mathbf{x}^{(j)} \leq c_{jk}) - \mathbb{V}(y \mid \mathbf{x}^{(j)} \leq c_{jk}) \right] \\ &= \frac{1}{\sigma^2} P(\mathbf{x}^{(j)} \leq c_{jk}) \left(\mathbb{E}(y \mid \mathbf{x}^{(j)} \leq c_{jk}) \right)^2 \end{aligned}$$

Similarly, the second term of equation (16) converges to

$$\begin{aligned} & \frac{1}{n} \frac{\tau n_{jk}^r}{\sigma^2 (\sigma^2 + \tau n_{jk}^r)} \left(\sum_{i: \mathbf{x}_i \in \mathcal{A}_R(j,k)} y_i^2 - \sum_{i: \mathbf{x}_i \in \mathcal{A}_R(j,k)} (y_i - \bar{y}_r)^2 \right) \\ &\rightarrow \frac{1}{\sigma^2} P(\mathbf{x}^{(j)} > c_{jk}) \left(\mathbb{E}(y \mid \mathbf{x}^{(j)} > c_{jk}) \right)^2 \end{aligned}$$

Taken together, as $n \rightarrow \infty$,

$$L_n(c_{jk}) \rightarrow \frac{1}{\sigma^2} \left[P(\mathbf{x}^{(j)} \leq c_{jk}) \left(\mathbb{E}(y \mid \mathbf{x}^{(j)} \leq c_{jk}) \right)^2 + P(\mathbf{x}^{(j)} > c_{jk}) \left(\mathbb{E}(y \mid \mathbf{x}^{(j)} > c_{jk}) \right)^2 \right].$$

D Complete simulation results

We compare to leading machine learning algorithms: random forests, gradient boosting machines, neural networks. All implementations had an R interface and were the current fastest implementations to our knowledge: `ranger` (Wright and Ziegler, 2015), `xgboost` (Chen and Guestrin, 2016), and `Keras` (Chollet et al., 2015) respectively. For `Keras` we used a single architecture but varied the number of training epochs depending on the noise

level of the problem. For `xgboost` we consider two specifications, one using the software defaults and another determined by a 5-fold cross-validated grid optimization (see Table 5); a reduced grid of parameter values was used at sample sizes $n > 10,000$.

Parameter name	$N = 10K$	$N > 10K$
<code>eta</code>	{0.1, 0.3}	{0.1, 0.3}
<code>max_depth</code>	{4, 8, 12}	{4, 12}
<code>colsample_bytree</code>	{0.7, 1}	{0.7, 1}
<code>min_child_weight</code>	{1, 10, 15}	10
<code>subsample</code>	0.8	0.8
<code>gamma</code>	0.1	0.1

Table 5: Hyperparameter Grid for `xgboost`.

The software used is R version 4.0.3 with `xgboost` 0.71.2, `dbarts` version 0.9.1, `ranger` 0.11.1 and `keras` 2.3.0.0. The default choice of hyperparameters for `xgboost` are `eta` = 0.3, `colsample_bytree` = 1, `min_child_weight` = 1 and `max_depth` = 6. `Ranger` was fit with `num.trees` = 500 and `mtry` = $\text{floor}(\sqrt{p})$. For `Keras` we build a network with two fully connected hidden layers (15 nodes each) using ReLU activation function, L_1 regularization at 0.01, and with 50/20 epochs depending on the signal to noise ratio. The simulation was ran on a cluster with two Intel Xeon Gold 6230 CPU and 320GB memory.

The tables below demonstrate simulation results of XBART, XGBoost with cross validation (XGBCV), XGBoost default parameters (XGB), random forests (RF) and neural networks (NN), on several different settings, including independent regressors (Table 6), correlated regressors (Table 7) and fat-tail error (Table 8).

Note that we consider XBART in two cases, fixed $\tau = \text{Var}(y)/L$, or assign an inverse-Gamma($3, 0.5 \times \text{Var}(y)/L$) and update τ in between of sweeps. In general, sampling τ improves the performance dramtically on high noise cases $\kappa = 10$, but the RMSE is slightly higher for the huge n cases such as $n = 250k, \kappa = 1$.

		$\kappa = 1$						$\kappa = 10$					
p	n	XBART fixed τ	XBART sampling τ	XGBCV	XGB	RF	NN	XBART fixed τ	XBART sampling τ	XGBCV	XGB	RF	NN
Linear													
500	300	25.94 (3.7)	25.38 (3.8)	27.16 (3.8)	28.53 (0.1)	24.87 (0.1)	24.14 (2.5)	53.42 (3.6)	33.7 (3.3)	78.2 (3.8)	112.24 (0.1)	33.08 (0.1)	26.57 (1.3)
100	1k	10.12 (2.1)	10.11 (1.9)	9.97 (7)	10.70 (0.1)	10.37 (0.2)	12.41 (27)	18.55 (1.6)	14.27 (1.5)	26.56 (7.1)	50.71 (0.1)	16.03 (0.2)	67.26 (11.0)
1k	500	35.57 (8.5)	35.39 (8.7)	36.07 (11)	40.08 (0.3)	35.04 (0.2)	34.23 (40.3)	67.68 (8.4)	45.87 (8.4)	103.55 (11.2)	148.6 (0.3)	49.95 (0.3)	172.04 (16.7)
1k	1k	35.81 (11.3)	35.5 (13.5)	36.27 (21.3)	39.86 (0.6)	35.21 (0.4)	31.93 (28)	59.15 (10.6)	44.88 (12.1)	85.86 (21.5)	161.2 (0.6)	43.31 (0.4)	208.87 (11.7)
30	10k	2.14 (8.1)	2.12 (5.5)	3.09 (28.0)	3.23 (0.3)	3.63 (1.0)	1.32 (27.3)	4.98 (3.4)	4.71 (4.0)	6.26 (25.8)	15.46 (0.2)	5.99 (1.1)	7.12 (11.2)
30	50k	1.46 (58.4)	1.43 (45.3)	2.93 (52.7)	2.69 (1.2)	3.31 (7.3)	0.66 (28.9)	3.90 (18.2)	3.60 (16.5)	4.48 (51.1)	9.22 (1.2)	4.77 (9.2)	3.53 (12.3)
30	250k	0.89 (639.5)	0.91 (406.1)	2.75 (540.1)	2.45 (11)	3.03 (59.7)	0.29 (37.1)	2.91 (222.7)	2.72 (153.0)	3.91 (504.1)	5.40 (10.9)	4.11 (83.8)	1.87 (15.8)
Max													
500	300	1.46 (3.8)	1.46 (3.3)	1.36 (3.8)	1.46 (0.1)	1.84 (0.1)	2.5 (2.6)	4.43 (3.6)	2.55 (3.5)	7.12 (3.9)	10.63 (0.1)	2.74 (0.1)	5.62 (1.4)
100	1k	0.92 (1.8)	0.91 (1.5)	0.92 (7.5)	1.2 (0.1)	1.43 (0.2)	2.67 (27.0)	3.62 (1.6)	2.57 (1.6)	5.06 (7.2)	9.88 (0.2)	2.98 (0.2)	16.48 (11.1)
1k	500	1.15 (8.8)	1.17 (8.5)	1.10 (11.4)	1.43 (0.3)	1.97 (0.3)	2.25 (40.6)	3.88 (8.4)	2.64 (8.5)	6.01 (10.8)	9.38 (0.3)	2.54 (0.2)	10.85 (16.5)
1k	1k	0.91 (11.6)	0.94 (15.4)	0.97 (21.7)	1.28 (0.6)	1.99 (0.5)	2.33 (27.9)	3.48 (10.6)	2.34 (12.4)	5.28 (21.4)	9.72 (0.6)	2.67 (0.4)	12.94 (11.5)
30	10k	0.40 (3.9)	0.40 (2.3)	0.44 (26.5)	0.62 (0.2)	0.61 (1.1)	0.42 (28.4)	1.60 (3.1)	1.54 (2.6)	2.03 (25.4)	5.46 (0.2)	2.14 (1.1)	3.1 (11.3)
30	50k	0.23 (17.7)	0.23 (10.4)	0.33 (52.9)	0.34 (1.1)	0.40 (8.8)	0.25 (28.8)	0.95 (13.0)	0.96 (12.9)	1.06 (48.9)	2.90 (1.1)	1.66 (9.3)	1.66 (12.0)
30	250k	0.14 (166.4)	0.15 (65.5)	0.24 (513.3)	0.20 (11.8)	0.27 (91.6)	0.18 (37.3)	0.58 (119.9)	0.58 (83.0)	0.62 (503)	1.46 (10.8)	1.37 (104.4)	0.81 (15.9)
Single Index													
500	300	6.18 (3.8)	6.22 (3.5)	8.11 (3.6)	8.19 (0.1)	8.40 (0.1)	20.43 (2.6)	19.76 (3.7)	14.7 (3.3)	26.82 (3.9)	40.52 (0.1)	12.23 (0.1)	34.81 (1.4)
100	1k	3.95 (1.8)	4.00 (1.7)	5.25 (7.1)	5.98 (0.1)	6.00 (0.2)	10.51 (26.9)	12.96 (1.6)	9.48 (1.5)	18.33 (7.3)	35.46 (0.1)	11.05 (0.2)	38.59 (11)
1k	500	4.84 (8.7)	4.75 (8.3)	7.17 (10.8)	7.59 (0.3)	7.89 (0.3)	14.07 (40.6)	14.65 (8.3)	10.14 (8.3)	23.81 (11.1)	38.53 (0.3)	11.6 (0.2)	39.23 (16.4)
1k	1k	4.08 (12.0)	4.12 (12.1)	5.93 (21.1)	6.78 (0.6)	7.86 (0.4)	12.01 (27.9)	12.96 (10.5)	9.98 (12.8)	20.41 (21.7)	35.02 (0.6)	10.54 (0.4)	50 (11.6)
30	10k	2.38 (5.8)	2.30 (4.4)	2.79 (25.5)	3.36 (0.3)	3.73 (1.1)	2.66 (27.5)	6.41 (3.2)	6.09 (2.6)	8.25 (25.4)	20.61 (0.2)	8.06 (1.1)	8.49 (11.2)
30	50k	1.68 (41.5)	1.66 (33.3)	2.22 (49.5)	2.35 (1.2)	3.08 (7.9)	1.96 (29.1)	4.45 (15.2)	4.41 (13.0)	5.51 (49.9)	11.71 (1.1)	6.62 (9.3)	6.45 (12.1)
30	250k	1.23 (518.4)	1.22 (326.6)	1.99 (489.2)	1.81 (11.0)	2.59 (73.0)	1.65 (37.8)	3.11 (176.3)	2.98 (116.9)	4.58 (508.5)	6.37 (9.7)	5.62 (94.4)	4.61 (16.0)
Trig+Poly													
500	300	4.39 (3.9)	5.03 (3.3)	5.20 (3.9)	5.74 (0.1)	5.41 (0.1)	7.08 (2.6)	12.02 (3.6)	7.84 (3.3)	15.34 (3.9)	25.23 (0.1)	7.56 (0.1)	9.55 (1.3)
100	1k	3.00 (1.8)	3.14 (1.6)	3.82 (7.3)	4.39 (0.2)	4.70 (0.2)	9.18 (27)	8.71 (1.6)	6.23 (1.5)	12.87 (7.3)	25.29 (0.1)	7.59 (0.2)	37.80 (11.1)
1k	500	3.26 (9.0)	3.13 (8.5)	4.18 (11.3)	4.54 (0.3)	5.01 (0.2)	6.46 (40.5)	9.81 (8.4)	6.32 (8.3)	14.6 (11.0)	23.34 (0.3)	6.22 (0.2)	26.66 (16.5)
1k	1k	2.90 (12.2)	2.85 (13.3)	4.04 (21.8)	4.74 (0.6)	5.21 (0.5)	7.22 (27.8)	9.27 (10.7)	6.43 (12.1)	13.29 (21.3)	23.37 (0.6)	6.36 (0.5)	33.26 (11.6)
30	10k	1.25 (5.0)	1.52 (3.9)	2.42 (26)	2.77 (0.2)	3.26 (1.1)	3.73 (27.3)	4.57 (3.1)	4.53 (2.6)	5.61 (25.4)	13.62 (0.2)	5.89 (1.2)	7.72 (11.3)
30	50k	0.74 (27.4)	0.75 (15.0)	2.30 (49.9)	1.96 (1.1)	2.83 (9.2)	3.26 (29.0)	3.06 (14.3)	3.07 (12.8)	4.02 (48.3)	7.44 (1.1)	4.92 (9.5)	5.56 (12.3)
30	250k	0.48 (273.1)	0.50 (134.3)	1.72 (504.3)	1.18 (10.8)	2.45 (93.1)	2.20 (37.6)	2.28 (146.6)	2.01 (104.4)	3.35 (507.1)	4.22 (9.7)	4.24 (103.6)	4.12 (16.2)

Table 6: Root mean squared error (RMSE) and running time in seconds (in parenthesis). Column p and n are number of regressors and observations respectively. Regressors X independent and the noise ϵ is Gaussian. The left panel is for noise level $\kappa = 1$ and the right panel is for higher noise level $\kappa = 10$.

		$\kappa = 1$						$\kappa = 10$					
p	n	XBART fixed τ	XBART sampling τ	XGBCV	XGB	RF	NN	XBART fixed τ	XBART sampling τ	XGBCV	XGB	RF	NN
Linear													
500	300	40.11 (3.9)	40.32 (3.5)	40.22 (3.9)	44.36 (0.1)	38.62 (0.1)	28.90 (2.7)	94.38 (3.7)	65.83 (3.4)	122.51 (3.8)	190.81 (0.1)	63.50 (0.1)	41.00 (1.3)
100	1k	15.33 (2.0)	15.37 (1.7)	12.57 (7.3)	13.73 (0.2)	13.23 (0.2)	19.19 (26.9)	33.48 (1.6)	21.15 (1.6)	43.43 (7.1)	77.66 (0.2)	21.41 (0.2)	101.98 (11.1)
1k	500	61.64 (8.5)	60.73 (9.5)	61.16 (10.8)	65.83 (0.3)	58.92 (0.2)	45.1 (40.7)	121.94 (8.5)	74.34 (9.4)	174.87 (10.9)	272.60 (0.3)	78.78 (0.3)	290.26 (16.6)
1k	1k	58.97 (12.2)	58.70 (13.8)	58.44 (21.2)	63.90 (0.6)	56.76 (0.4)	45.48 (27.9)	97.75 (10.5)	71.13 (13.4)	153.25 (21.5)	283.11 (0.6)	72.73 (0.4)	369.02 (11.4)
30	10k	2.52 (7.0)	2.50 (5.6)	3.51 (27.8)	4.01 (0.3)	3.60 (1.0)	1.89 (27.5)	7.22 (3.3)	5.73 (2.7)	8.57 (25.9)	23.72 (0.2)	8.59 (1.1)	9.64 (11.6)
30	50k	1.73 (50.9)	1.74 (40.2)	2.88 (52.1)	3.14 (1.1)	3.13 (7.0)	0.86 (28.8)	4.80 (17.5)	4.26 (15.8)	5.30 (49.7)	13.06 (1.1)	6.46 (8.9)	4.44 (12.0)
30	250k	1.13 (614.3)	1.12 (313.0)	2.59 (495.6)	2.64 (7.9)	2.78 (57.9)	0.42 (38.3)	3.56 (222.7)	3.27 (133.3)	4.43 (498.1)	7.22 (16.2)	5.51 (82.8)	2.18 (15.6)
Max													
500	300	1.53 (3.9)	1.52 (3.4)	1.35 (3.9)	1.46 (0.1)	2.00 (0.1)	2.56 (2.7)	5.12 (3.8)	3.06 (3.3)	6.31 (3.8)	9.77 (0.1)	2.94 (0.1)	7.10 (1.3)
100	1k	0.94 (1.8)	0.92 (1.5)	0.87 (7.3)	1.22 (0.2)	1.46 (0.2)	2.82 (27.0)	3.40 (1.6)	2.60 (1.5)	5.32 (7.3)	9.70 (0.2)	3.28 (0.2)	15.59 (11.0)
1k	500	1.23 (9.0)	1.27 (9.8)	1.20 (11.1)	1.45 (0.3)	2.08 (0.3)	2.27 (40.8)	3.58 (8.4)	2.71 (9.6)	5.94 (10.7)	9.06 (0.3)	2.78 (0.2)	9.88 (16.7)
1k	1k	0.98 (11.3)	0.94 (13.3)	0.98 (21.9)	1.24 (0.6)	2.05 (0.5)	2.46 (28.3)	3.65 (10.3)	2.71 (14.1)	5.36 (21.2)	9.25 (0.6)	2.71 (0.5)	13.27 (11.7)
30	10k	0.43 (4.0)	0.44 (2.2)	0.45 (27.1)	0.68 (0.2)	0.73 (1.1)	0.44 (27.7)	1.73 (3.1)	1.62 (2.6)	2.22 (25.6)	5.86 (0.2)	2.30 (1.1)	2.98 (11.4)
30	50k	0.24 (18.1)	0.26 (9.4)	0.37 (51.5)	0.38 (1.1)	0.50 (8.2)	0.23 (29.1)	1.05 (13.1)	1.08 (11.9)	1.18 (49.5)	3.11 (1.1)	1.80 (9.1)	1.75 (11.9)
30	250k	0.16 (171.4)	0.17 (66.8)	0.27 (491.2)	0.21 (7.7)	0.36 (86.4)	0.22 (36.8)	0.65 (125.4)	0.63 (88.9)	0.67 (534.6)	1.61 (15.1)	1.49 (97.4)	0.90 (21.8)
Single Index													
500	300	5.41 (3.8)	5.35 (3.3)	7.86 (3.7)	7.94 (0.1)	8.22 (0.1)	19.49 (2.6)	19.27 (3.7)	12.72 (3.3)	26.03 (3.8)	40.03 (0.1)	11.76 (0.1)	32.54 (1.3)
100	1k	4.08 (1.8)	4.08 (1.6)	5.56 (7.1)	6.38 (0.2)	6.32 (0.2)	10.04 (27.2)	12.72 (1.6)	9.43 (1.5)	20.03 (7.2)	38.18 (0.1)	11.68 (0.2)	34.88 (11.1)
1k	500	4.80 (8.7)	4.78 (8.2)	6.57 (10.4)	7.49 (0.3)	7.92 (0.2)	13.63 (40.6)	14.94 (8.4)	10.91 (8.3)	24.31 (10.9)	37.17 (0.3)	10.23 (0.2)	41.36 (16.4)
1k	1k	3.97 (12.1)	3.92 (12.6)	5.92 (21.1)	6.48 (0.6)	7.51 (0.4)	12.29 (28.0)	12.43 (10.9)	9.91 (13.8)	20.45 (21.4)	35.57 (0.6)	9.99 (0.5)	50.13 (11.5)
30	10k	2.53 (5.4)	2.58 (3.5)	3.10 (26.0)	3.78 (0.2)	3.73 (1.0)	3.17 (27.4)	7.30 (3.2)	6.88 (2.6)	9.46 (25.7)	25.15 (0.2)	9.73 (1.1)	9.59 (11.3)
30	50k	1.80 (38.9)	1.80 (29.3)	2.41 (50.4)	2.64 (1.2)	3.08 (7.6)	2.10 (28.7)	4.73 (15.1)	4.62 (13.4)	5.71 (49.8)	13.86 (1.1)	7.44 (9.3)	6.44 (12.0)
30	250k	1.31 (532.7)	1.34 (331.2)	2.16 (522.6)	2.08 (7.9)	2.60 (74.8)	1.75 (38.7)	3.43 (187.7)	3.36 (118.7)	4.48 (521.6)	7.50 (11.3)	6.43 (109.6)	4.61 (15.6)
Trig+Poly													
500	300	3.72 (3.9)	4.13 (3.4)	4.72 (3.8)	5.16 (0.1)	4.96 (0.1)	6.71 (2.6)	11.26 (3.6)	7.43 (3.3)	17.45 (3.9)	24.04 (0.1)	7.85 (0.1)	10.06 (1.4)
100	1k	2.89 (1.8)	2.78 (1.5)	3.68 (7.3)	4.43 (0.2)	4.64 (0.2)	9.44 (27.1)	8.12 (1.6)	6.20 (1.5)	12.42 (7.1)	24.91 (0.1)	7.80 (0.2)	36.26 (11.0)
1k	500	3.58 (8.9)	3.53 (9.9)	4.72 (11.0)	5.00 (0.3)	5.14 (0.2)	6.40 (40.5)	10.51 (8.3)	7.71 (8.3)	14.19 (10.8)	23.39 (0.3)	6.99 (0.2)	25.79 (16.4)
1k	1k	2.92 (12.1)	3.02 (12.3)	4.28 (21.8)	4.80 (0.6)	5.26 (0.5)	7.24 (27.8)	8.04 (10.4)	6.48 (13.2)	12.73 (21.4)	23.55 (0.6)	6.72 (0.5)	32.92 (11.5)
30	10k	1.24 (5.1)	1.21 (4.1)	1.99 (26.0)	2.27 (0.2)	2.96 (1.1)	3.59 (27.4)	4.80 (3.2)	4.88 (2.7)	5.88 (25.4)	14.02 (0.2)	6.24 (1.1)	7.70 (11.3)
30	50k	0.75 (28.4)	0.80 (17.3)	1.36 (49.8)	1.42 (1.1)	2.23 (8.5)	2.66 (28.7)	3.01 (14.4)	3.05 (13.2)	3.83 (49.1)	7.65 (1.1)	4.87 (9.2)	5.43 (12)
30	250k	0.50 (336.4)	0.51 (152.1)	1.26 (498)	1.05 (7.6)	1.71 (81.5)	0.96 (36.9)	2.00 (167.1)	1.88 (94.3)	2.71 (496.9)	4.05 (7.7)	3.99 (112.7)	4.27 (15.6)

Table 7: Root mean squared error (RMSE) and running time in seconds (in parenthesis). Column p and n are number of regressors and observations respectively. Regressors X are correlated with factor structure and the noise ϵ is Gaussian. The left panel is for noise level $\kappa = 1$ and the right panel is for higher noise level $\kappa = 10$.

		$\kappa = 1$						$\kappa = 10$					
p	n	XBART fixed τ	XBART sampling τ	XGBCV	XGB	RF	NN	XBART fixed τ	XBART sampling τ	XGBCV	XGB	RF	NN
Linear													
500	300	25.42 (3.9)	25.13 (3.3)	25.70 (3.8)	28.31 (0.1)	25.03 (0.1)	24.24 (2.7)	48.86 (3.7)	34.46 (3.5)	73.34 (3.9)	144.63 (0.1)	40.43 (0.2)	27.04 (1.3)
100	1k	9.88 (2.1)	9.87 (1.7)	9.39 (7.7)	9.87 (0.2)	9.76 (0.2)	12.52 (27.0)	18.08 (1.7)	12.55 (1.6)	25.73 (7.4)	48.01 (0.1)	17.42 (0.2)	58.65 (11.0)
1k	500	37.09 (8.6)	36.31 (8.4)	37.95 (11.3)	39.16 (0.3)	35.71 (0.2)	33.95 (40.9)	41.29 (8.6)	37.49 (8.5)	46.34 (11.6)	62.18 (0.3)	36.9 (0.2)	56.26 (16.6)
1k	1k	36.01 (11.8)	35.53 (14.8)	36.75 (22.1)	38.39 (0.6)	35.14 (0.5)	31.46 (28.2)	58.62 (10.8)	42.3 (13.3)	87.26 (22)	153.16 (0.6)	45.97 (0.5)	199.86 (11.5)
30	10k	2.13 (8.2)	2.14 (5.7)	3.17 (26.9)	3.29 (0.3)	3.68 (1.0)	1.37 (27.2)	5.34 (3.4)	4.81 (2.8)	7.11 (24.5)	16.37 (0.2)	6.73 (1.2)	7.08 (11.3)
30	50k	1.44 (59.7)	1.49 (44.1)	2.93 (52.4)	2.75 (1.2)	3.31 (7.1)	0.60 (28.8)	3.82 (18.5)	3.60 (16.9)	5.08 (48.8)	10.72 (1.1)	5.12 (9.6)	3.56 (12.0)
30	250k	0.91 (633.1)	1.04 (406.2)	2.8 (483.3)	2.52 (8.2)	3.02 (59.0)	0.34 (37.6)	3.18 (221.8)	3.90 (170.3)	5.01 (469.1)	8.29 (9.1)	4.31 (90.1)	1.89 (15.8)
Max													
500	300	1.48 (3.9)	1.53 (3.4)	1.32 (3.8)	1.54 (0.1)	1.94 (0.1)	2.57 (2.6)	4.85 (3.7)	3.06 (3.5)	6.77 (4.0)	10.84 (0.1)	3.39 (0.1)	5.48 (1.3)
100	1k	0.81 (1.8)	0.79 (1.5)	0.82 (7.6)	1.14 (0.1)	1.35 (0.2)	2.68 (26.7)	3.35 (1.6)	2.46 (1.5)	5.07 (7.3)	10.64 (0.1)	3.79 (0.2)	15.17 (11)
1k	500	1.27 (9.1)	1.24 (8.6)	1.17 (11.5)	1.46 (0.3)	1.98 (0.3)	2.25 (40.7)	1.97 (8.6)	1.79 (8.4)	2.49 (11.2)	4.10 (0.3)	2.14 (0.3)	3.71 (16.6)
1k	1k	0.80 (12.1)	0.81 (13.4)	0.86 (22.9)	1.24 (0.6)	1.89 (0.5)	2.31 (27.8)	3.28 (10.6)	2.32 (13.5)	5.30 (22.2)	9.77 (0.6)	2.90 (0.5)	12.29 (11.5)
30	10k	0.40 (4.0)	0.44 (2.1)	0.46 (25.6)	0.66 (0.2)	0.59 (1.2)	0.38 (27.1)	1.66 (3.1)	1.55 (2.5)	2.15 (24.3)	5.80 (0.2)	2.47 (1.2)	2.84 (11.4)
30	50k	0.24 (18.5)	0.28 (9.4)	0.34 (50.1)	0.41 (1.1)	0.38 (9.2)	0.24 (28.7)	1.00 (13.7)	1.40 (11.7)	1.20 (47.7)	3.58 (1.1)	1.88 (10.1)	1.56 (11.9)
30	250k	0.15 (161.9)	0.18 (69.1)	0.26 (448.2)	0.23 (7.8)	0.25 (91.8)	0.19 (37.9)	0.58 (119.7)	0.59 (87.5)	0.70 (464.7)	1.75 (7.8)	1.47 (108.7)	0.82 (15.8)
Single Index													
500	300	5.46 (3.8)	5.41 (3.3)	7.61 (3.8)	8.41 (0.1)	8.02 (0.1)	18.94 (2.8)	20.39 (3.7)	14.07 (3.4)	29.98 (4.1)	35.83 (0.1)	13.96 (0.1)	33.75 (1.3)
100	1k	4.34 (1.8)	4.17 (1.6)	5.55 (6.9)	6.32 (0.1)	6.28 (0.2)	10.31 (27.0)	13.60 (1.7)	9.66 (1.7)	18.33 (7.2)	36.31 (0.2)	13.88 (0.2)	35.01 (11.1)
1k	500	4.77 (8.8)	4.74 (9.6)	6.91 (10.5)	7.68 (0.3)	8.13 (0.3)	13.47 (40.9)	6.94 (8.7)	6.84 (8.1)	10.93 (11.5)	13.47 (0.3)	8.68 (0.3)	19.72 (16.6)
1k	1k	4.01 (11.9)	3.87 (14.3)	6.05 (21.1)	6.67 (0.6)	7.69 (0.5)	12.58 (28.0)	13.42 (10.6)	9.74 (11.9)	19.77 (22.1)	34.75 (0.6)	11.13 (0.5)	45.43 (11.5)
30	10k	2.37 (5.9)	2.46 (4.9)	2.81 (24.9)	3.32 (0.2)	3.65 (1.1)	2.69 (27.4)	6.40 (3.3)	7.06 (2.4)	8.78 (24.9)	23.68 (0.2)	9.74 (1.2)	9.28 (11.4)
30	50k	1.65 (42.5)	2.46 (31.3)	2.26 (49.0)	2.47 (1.1)	3.05 (8.2)	1.93 (28.9)	4.58 (15.7)	12.21 (11.6)	6.51 (48.3)	14.23 (1.1)	7.29 (9.8)	6.45 (11.9)
30	250k	1.22 (524.5)	1.28 (352.7)	2.01 (455.1)	1.89 (7.9)	2.53 (83.2)	1.68 (37.2)	3.17 (179.0)	3.06 (117.5)	4.75 (468.5)	7.85 (8.6)	6.00 (101.6)	4.66 (16.0)
Trig+Poly													
500	300	4.22 (3.9)	4.42 (3.3)	4.89 (3.7)	5.20 (0.1)	5.24 (0.1)	6.41 (2.6)	11.48 (3.7)	7.40 (3.4)	14.05 (4.0)	31.32 (0.1)	7.61 (0.1)	7.19 (1.4)
100	1k	2.80 (1.8)	2.90 (1.5)	3.68 (7.3)	4.27 (0.2)	4.60 (0.2)	9.14 (26.9)	8.36 (1.6)	6.21 (1.5)	12.82 (7.3)	29.21 (0.1)	9.64 (0.2)	33.32 (11.0)
1k	500	3.89 (9.2)	4.03 (8.7)	4.89 (11.5)	5.75 (0.3)	5.34 (0.3)	6.74 (40.5)	5.98 (8.7)	5.64 (9.5)	7.01 (11.6)	12.71 (0.3)	5.71 (0.3)	9.98 (16.6)
1k	1k	2.86 (11.9)	2.93 (12.5)	4.11 (21.8)	4.88 (0.6)	5.24 (0.5)	7.02 (28.2)	8.81 (10.5)	6.79 (11.6)	13.44 (22.3)	27.91 (0.6)	7.91 (0.5)	33.00 (11.5)
30	10k	1.22 (5.0)	1.27 (2.9)	2.46 (25.7)	2.39 (0.2)	3.28 (1.2)	3.95 (27.4)	4.66 (3.2)	4.78 (2.5)	6.02 (24.6)	13.07 (0.2)	6.65 (1.2)	7.94 (11.3)
30	50k	0.77 (28.4)	1.30 (14.5)	2.23 (48.5)	2.02 (1.1)	2.86 (9.5)	3.62 (28.9)	3.36 (13.8)	3.79 (11.0)	4.23 (47.3)	8.33 (1.1)	5.29 (10.1)	5.43 (12.2)
30	250k	1.77 (247.8)	1.53 (121.9)	1.87 (481.3)	1.82 (7.7)	2.48 (95.8)	2.36 (37.3)	2.37 (136.8)	2.89 (100.0)	3.59 (466.5)	5.86 (7.9)	4.51 (110.8)	4.21 (15.8)

Table 8: Root mean squared error (RMSE) and running time in seconds (in parenthesis). Column p and n are number of regressors and observations respectively. Regressors X are independent and the noise ϵ is t distributed with degree of freedom 3. The left panel is for noise level $\kappa = 1$ and the right panel is for higher noise level $\kappa = 10$.

**Supplementary material for
Stochastic tree ensembles for regularized nonlinear
regression**

**A Connection between XBART and CART theoretical split
criterion, Condition 1**

In this section, we first establish the connection between theoretical split criterion of XBART and that of CART. Suppose the current parent node is \mathcal{A} , the XBART theoretical split criterion of cutpoint candidate c_{jk} is

$$L_{\text{XBART}}^*(c_{jk}) = \frac{1}{\sigma^2} \mathbb{P}(x^{(i)} \leq c_{jk} \mid \mathbf{x} \in \mathcal{A}) \left[\mathbb{E}(Y \mid x^{(i)} \leq c_{jk}, \mathbf{x} \in \mathcal{A}) \right]^2 \\ + \frac{1}{\sigma^2} \mathbb{P}(x^{(i)} > c_{jk} \mid \mathbf{x} \in \mathcal{A}) \left[\mathbb{E}(Y \mid x^{(i)} > c_{jk}, \mathbf{x} \in \mathcal{A}) \right]^2.$$

The CART theoretical split criterion is

$$L_{\text{CART}}^*(c_{jk}) = \mathbb{V}(Y \mid \mathbf{x} \in \mathcal{A}) - \mathbb{P}(x^{(j)} \leq c_{jk} \mid \mathbf{x} \in \mathcal{A}) \mathbb{V}(Y \mid x^{(j)} \leq c_{jk}, \mathbf{x} \in \mathcal{A}) \\ - \mathbb{P}(x^{(j)} > c_{jk} \mid \mathbf{x} \in \mathcal{A}) \mathbb{V}(Y \mid x^{(j)} > c_{jk}, \mathbf{x} \in \mathcal{A}).$$

Recall that the cuts are always parallel to axis,

$$\mathbb{V}(Y \mid x^{(j)} \leq c_{jk}, \mathbf{x} \in \mathcal{A}) = \mathbb{E}(Y^2 \mid x^{(j)} \leq c_{jk}, \mathbf{x} \in \mathcal{A}) - \left[\mathbb{E}(Y \mid x^{(j)} \leq c_{jk}, \mathbf{x} \in \mathcal{A}) \right]^2.$$

We have

$$\mathbb{E}(Y^2 \mid x^{(j)} \leq c_{jk}, \mathbf{x} \in \mathcal{A}) = \frac{1}{\Omega(\{x^{(j)} \leq c_{jk}, \mathbf{x} \in \mathcal{A}\})} \int_{\mathbf{x} \in \{x^{(j)} \leq c_{jk}, \mathbf{x} \in \mathcal{A}\}} m^2(\mathbf{x}) d\mathbf{x},$$

where $\Omega(\mathcal{A})$ represents volume of the cube \mathcal{A} . Observe that

$$\mathbb{P}(x^{(j)} \leq c_{jk} \mid \mathbf{x} \in \mathcal{A}) = \frac{\Omega(\{x^{(j)} \leq c_{jk}, \mathbf{x} \in \mathcal{A}\})}{\Omega(\mathcal{A})},$$

it yields

$$\begin{aligned}
& \mathbb{E}(Y^2 \mid \mathbf{x} \in \mathcal{A}) - \mathbb{P}(\mathbf{x}^{(j)} \leq c_{jk} \mid \mathbf{x} \in \mathcal{A})\mathbb{E}(Y^2 \mid \mathbf{x}^{(j)} \leq c_{jk}, \mathbf{x} \in \mathcal{A}) \\
& \quad - \mathbb{P}(\mathbf{x}^{(j)} > c_{jk} \mid \mathbf{x} \in \mathcal{A})\mathbb{E}(Y^2 \mid \mathbf{x}^{(j)} > c_{jk}, \mathbf{x} \in \mathcal{A}) \\
&= \frac{1}{\Omega(\mathcal{A})} \int_{\mathbf{x} \in \mathcal{A}} m^2(\mathbf{x}) d\mathbf{x} - \frac{1}{\Omega(\mathcal{A})} \int_{\mathbf{x} \in \{\mathbf{x}^{(j)} \leq c_{jk}, \mathbf{x} \in \mathcal{A}\}} m^2(\mathbf{x}) d\mathbf{x} - \frac{1}{\Omega(\mathcal{A})} \int_{\mathbf{x} \in \{\mathbf{x}^{(j)} > c_{jk}, \mathbf{x} \in \mathcal{A}\}} m^2(\mathbf{x}) d\mathbf{x} \\
&= 0.
\end{aligned}$$

As a result, the CART theoretical split criterion is equivalent to

$$\begin{aligned}
L_{\text{CART}}^*(c_{jk}) &= [\mathbb{E}(Y \mid \mathbf{x} \in \mathcal{A})]^2 - \mathbb{P}(\mathbf{x}^{(i)} \leq c_{jk} \mid \mathbf{x} \in \mathcal{A}) \left[\mathbb{E}(Y \mid \mathbf{x}^{(i)} \leq c_{jk}, \mathbf{x} \in \mathcal{A}) \right]^2 \\
& \quad - \mathbb{P}(\mathbf{x}^{(i)} > c_{jk} \mid \mathbf{x} \in \mathcal{A}) \left[\mathbb{E}(Y \mid \mathbf{x}^{(i)} > c_{jk}, \mathbf{x} \in \mathcal{A}) \right]^2 \\
&= [\mathbb{E}(Y \mid \mathbf{x} \in \mathcal{A})]^2 - \sigma^2 L_{\text{XBART}}^*(c_{jk}).
\end{aligned}$$

Since $[\mathbb{E}(Y \mid \mathbf{x} \in \mathcal{A})]^2$ and σ^2 are constants, and we maximize $L_{\text{XBART}}^*(c_{jk})$ but minimize $L_{\text{CART}}^*(c_{jk})$ in practice, we claim that the two theoretical split criterion are equivalent.

[Scornet et al. \(2015\)](#) show that Condition 1 (their Lemma 1) is valid under the assumption of f below

Assumption 1 (A1).

$$y = \sum_{k=1}^p f^{(k)}(\mathbf{x}^{(k)}) + \epsilon,$$

where $\mathbf{x} = (\mathbf{x}^{(1)}, \dots, \mathbf{x}^{(p)})$ is uniformly distributed on $[0, 1]^p$. $\epsilon \sim N(0, s^2)$. Each $f^{(k)}(x)$ is continuous on $[0, 1]$.

Since the theoretical split criterion of CART and XBART are equivalent, their proof applies directly without modification to XBART under the same Assumption (A1). We refer readers to [Scornet et al. \(2015\)](#) for details.

However, a weaker replacement of Assumption (A1) is to assume Condition 1 is valid directly, with extra assumption $\|f\|_\infty < \infty$, continuous on $[0, 1]^p$. Although this is perhaps less interpretable than an assumption of an additive model, it is also presumably a weaker assumption in that it may be satisfied by non-additive models. Therefore in our paper, we assume Condition 1 is valid rather than Assumption A1.

B Proof of Lemma 1

Essentially the proof shows that adding small perturbation $\mathbf{c}'_k = (c'_1, \dots, c'_k)$ to the **sequence** of cutpoints $\mathbf{c}_k = (c_1, \dots, c_k)$, the change of split criterion at the bottom node $|L_{n,k}(x, \mathbf{c}'_k) - L_{n,k}(x, \mathbf{c}_k)|$ is small. In the proof, we should two different bounding strategies as follows,

S1 Perturb cutpoint of the **parent** of the bottom node.

S2 Perturb cutpoint of **nodes above the parent** (two levels above, or higher) of the bottom node.

We show that **S1** and **S2** are valid first, in the setting of $k = 1$ and $k = 2$, and demonstrate proof for general k with the two strategies.

B.1 Bounding strategy S1, Proof of Lemma 1 for the case $k = 1$

In this section, we start from S1, bounding the variation when perturb cutpoint of the parent node. Without loss of generality, we assume $k = 1$ and consider the first cut at the root node. Note that the case $L_{n,1}(x, \cdot)$ does not depend on x , we write $L_{n,1}(\cdot)$ instead of $L_{n,1}(x, \cdot)$.

Preliminary results Let $Z_i = \max_{1 \leq i \leq n} |\epsilon_i|$, we have

$$\mathbb{P}(Z_i \geq t) = 1 - \exp[n \ln(1 - 2\mathbb{P}(\epsilon_i \geq t))].$$

The tail of Gaussian distribution has a standard bound:

$$\mathbb{P}(\epsilon_i \geq t) \leq \frac{\sigma}{t\sqrt{2\pi}} \left(-\frac{t^2}{2\sigma^2} \right).$$

As a result, there exist a positive constant C_ρ and $N_1 \in \mathbb{N}^*$ such that with probability $1 - \rho$, for all $n > N_1$,

$$\max_{1 \leq i \leq n} |\epsilon_i| \leq C_\rho \sqrt{\log(n)}.$$

In addition, we have

$$\mathbb{P} \left[\left| \frac{1}{n} \sum_{i=1}^n \epsilon_i \right| \geq \alpha \right] \leq \frac{\sigma}{\alpha \sqrt{n}} \exp \left(-\frac{\alpha^2 n}{2\sigma^2} \right).$$

Let $N_n(A)$ denotes number of data observations in a set A . Next we derive from the inequality above and union bound inequality that there exists $N_2 \in \mathbb{N}^*$ such that with probability $1 - \rho$, for all $n > N_2$ and all $0 \leq a_n \leq b_n \leq 1$ satisfying $N_n([a_n, b_n] \times [0, 1]^{p-1}) > \sqrt{n}$,

$$\left| \frac{1}{N_n([a_n, b_n] \times [0, 1]^{p-1})} \sum_{i: x_i \in [a_n, b_n] \times [0, 1]^{p-1}} \epsilon_i \right| \leq \alpha.$$

and

$$\frac{1}{N_n([a_n, b_n] \times [0, 1]^{p-1})} \sum_{i: x_i \in [a_n, b_n] \times [0, 1]^{p-1}} \epsilon_i^2 \leq \tilde{\sigma}^2.$$

Furthermore, it's easy to verify

$$\left| \frac{1}{N_n([a_n, b_n] \times [0, 1]^{p-1})} \sum_{i: x_i \in [a_n, b_n] \times [0, 1]^{p-1}} Y_i \right| \leq \|f\|_\infty + \alpha, \quad (17)$$

where f is the true function, and

$$\left| \frac{1}{N_n([a_n, b_n] \times [0, 1]^{p-1})} \sum_{i: x_i \in [a_n, b_n] \times [0, 1]^{p-1}} Y_i^2 \right| \leq \|f\|_\infty^2 + \tilde{\sigma}^2 + 2\alpha \|f\|_\infty. \quad (18)$$

By the Glivenko-Cantelli theorem, there exist $N_3 \in \mathbb{N}^*$ such that with probability $1 - \rho$, for all $0 \leq a \leq b \leq 1$ and all $n > N_3$,

$$(b - a - \delta^2)n \leq N_n([a_n, b_n] \times [0, 1]^{p-1}) \leq (b - a + \delta^2)n. \quad (19)$$

In the following proof, we assume to be on the event that all claims above holds with probability $1 - 3\rho$ for all $n > N = \max\{N_1, N_2, N_3\}$. Take $c_1, c_2 \in [0, 1]$ such that $|c_1 - c_2| < \delta$ and assume that $c_1 < c_2$. We partition the space $[0, 1]^p$ into several pieces as follows, see Figure 5 for an illustration of notations for $k = 1$, where we project the p dimensional cells

onto the first variable.

$$\begin{cases} A_{L,\sqrt{\delta}} = [0, \sqrt{\delta}] \times [0, 1]^{p-1} \\ A_{R,\sqrt{\delta}} = [1 - \sqrt{\delta}, 1] \times [0, 1]^{p-1} \\ A_{C,\sqrt{\delta}} = [\sqrt{\delta}, 1 - \sqrt{\delta}] \times [0, 1]^{p-1} \end{cases} .$$

Similarly,

$$\begin{cases} A_{L,1} = [0, c_1] \times [0, 1]^{p-1} \\ A_{R,1} = [c_1, 1] \times [0, 1]^{p-1} \\ A_{L,2} = [0, c_2] \times [0, 1]^{p-1} \\ A_{R,2} = [c_2, 1] \times [0, 1]^{p-1} \\ A_C = [c_1, c_2] \times [0, 1]^{p-1} \end{cases} .$$

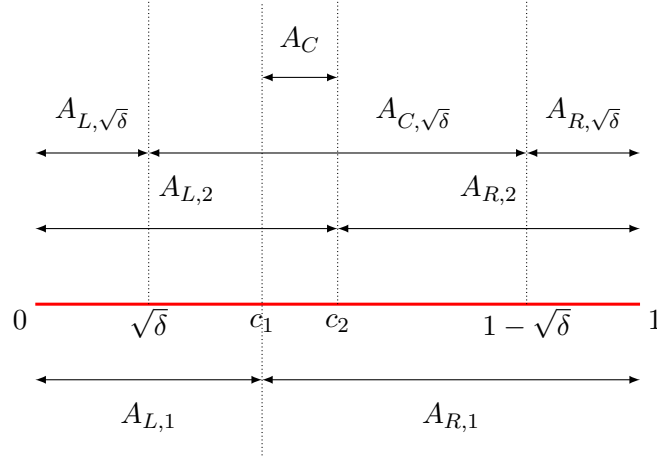


Figure 5: Illustration of notations for $k = 2$. Projection of the cells onto the first variable.

For simplicity, we write the split criterion of the first cut $\mathbf{c} = (1, c)$ as $L_{n,1}(1, c)$ denoting

split at the first variable and value c . Recall that our split criterion is defined as

$$\begin{aligned}
L_{n,1}(1, c) &= \frac{\tau N_n(A_L)}{\sigma^2(\sigma^2 + \tau N_n(A_L))} \frac{1}{n} \left(\sum_{i: x_i^{(1)} \leq c} y_i^2 - \sum_{i: x_i^{(1)} \leq c} (y_i - \bar{y}_l)^2 \right) \\
&+ \frac{\tau N_n(A_R)}{\sigma^2(\sigma^2 + \tau N_n(A_R))} \frac{1}{n} \left(\sum_{i: x_i^{(1)} > c} y_i^2 - \sum_{i: x_i^{(1)} > c} (y_i - \bar{y}_r)^2 \right) \\
&+ \frac{\gamma_x}{n}.
\end{aligned}$$

The difference of split criterion on two cutvalues c_1 and c_2 , on the first variable is

$$\begin{aligned}
&L_{n,1}(1, c_1) - L_{n,1}(1, c_2) \\
&= \frac{\tau N_n(A_{L,1})}{\sigma^2(\sigma^2 + \tau N_n(A_{L,1}))} \frac{1}{n} \left(\sum_{i: x_i^{(1)} \leq c_1} y_i^2 - \sum_{i: x_i^{(1)} \leq c_1} (y_i - \bar{y}_{A_{L,1}})^2 \right) \\
&\quad + \frac{\tau N_n(A_{R,1})}{\sigma^2(\sigma^2 + \tau N_n(A_{R,1}))} \frac{1}{n} \left(\sum_{i: x_i^{(1)} > c_1} y_i^2 - \sum_{i: x_i^{(1)} > c_1} (y_i - \bar{y}_{A_{R,1}})^2 \right) \\
&\quad - \frac{\tau N_n(A_{L,2})}{\sigma^2(\sigma^2 + \tau N_n(A_{L,2}))} \frac{1}{n} \left(\sum_{i: x_i^{(1)} \leq c_2} y_i^2 - \sum_{i: x_i^{(1)} \leq c_2} (y_i - \bar{y}_{A_{L,2}})^2 \right) \\
&\quad - \frac{\tau N_n(A_{R,2})}{\sigma^2(\sigma^2 + \tau N_n(A_{R,2}))} \frac{1}{n} \left(\sum_{i: x_i^{(1)} > c_2} y_i^2 - \sum_{i: x_i^{(1)} > c_2} (y_i - \bar{y}_{A_{R,2}})^2 \right) \\
&\quad + \frac{\gamma_{c_1}}{n} - \frac{\gamma_{c_2}}{n}.
\end{aligned} \tag{20}$$

We need to prove Lemma 1 for all possible cases depending on location of c_1 and c_2 . For notation simplicity, note that after collecting terms, the difference of split criterion can be represented as summation of points for the range of index $\{i : x_i^{(1)} < c_1\}$, $\{i : x_i^{(1)} \in [c_1, c_2]\}$ and $\{i : x_i^{(1)} > c_2\}$. We will use the same decomposition throughout the proof.

First case

Assume that $c_1, c_2 \in A_{C, \sqrt{\delta}}$, two cutpoint candidates are not close to the edge. Consider

the split criterion

$$\begin{aligned}
& L_{n,1}(1, c_1) - L_{n,1}(1, c_2) \\
&= \frac{\tau N_n(A_{L,1})}{\sigma^2(\sigma^2 + \tau N_n(A_{L,1}))} \frac{1}{n} \left(\sum_{i: x_i^{(1)} \leq c_1} y_i^2 - \sum_{i: x_i^{(1)} \leq c_1} (y_i - \bar{y}_{A_{L,1}})^2 \right) \\
&\quad + \frac{\tau N_n(A_{R,1})}{\sigma^2(\sigma^2 + \tau N_n(A_{R,1}))} \frac{1}{n} \left(\sum_{i: x_i^{(1)} > c_1} y_i^2 - \sum_{i: x_i^{(1)} > c_1} (y_i - \bar{y}_{A_{R,1}})^2 \right) \\
&\quad - \frac{\tau N_n(A_{L,2})}{\sigma^2(\sigma^2 + \tau N_n(A_{L,2}))} \frac{1}{n} \left(\sum_{i: x_i^{(1)} \leq c_2} y_i^2 - \sum_{i: x_i^{(1)} \leq c_2} (y_i - \bar{y}_{A_{L,2}})^2 \right) \\
&\quad - \frac{\tau N_n(A_{R,2})}{\sigma^2(\sigma^2 + \tau N_n(A_{R,2}))} \frac{1}{n} \left(\sum_{i: x_i^{(1)} > c_2} y_i^2 - \sum_{i: x_i^{(1)} > c_2} (y_i - \bar{y}_{A_{R,2}})^2 \right) \\
&\quad + \frac{\gamma_{c_1}}{n} - \frac{\gamma_{c_2}}{n} \\
&= J_1 + J_2 + J_3 + \frac{\gamma_{c_1}}{n} - \frac{\gamma_{c_2}}{n}.
\end{aligned}$$

First, take n large enough, we have

$$\left| \frac{\gamma_{c_1}}{n} - \frac{\gamma_{c_2}}{n} \right| \leq \alpha.$$

Let J_2 corresponding to $\{i \mid \mathbf{x}_i^{(1)} \in [c_1, c_2]\}$

$$\begin{aligned}
J_2 &= \frac{\tau N_n(A_{R,1})}{\sigma^2(\sigma^2 + \tau N_n(A_{R,1}))} \frac{1}{n} \left(\sum_{i:\mathbf{x}_i^{(1)} \in [c_1, c_2]} y_i^2 - \sum_{i:\mathbf{x}_i^{(1)} \in [c_1, c_2]} (y_i - \bar{y}_{A_{R,1}})^2 \right) \\
&\quad - \frac{\tau N_n(A_{L,2})}{\sigma^2(\sigma^2 + \tau N_n(A_{L,2}))} \frac{1}{n} \left(\sum_{i:\mathbf{x}_i^{(1)} \in [c_1, c_2]} y_i^2 - \sum_{i:\mathbf{x}_i^{(1)} \in [c_1, c_2]} (y_i - \bar{y}_{A_{L,2}})^2 \right) \\
&= \frac{\tau N_n(A_{R,1})}{\sigma^2(\sigma^2 + \tau N_n(A_{R,1}))} \left(\frac{1}{n} \sum_{i:\mathbf{x}_i^{(1)} \in [c_1, c_2]} y_i^2 \right) - \frac{\tau N_n(A_{L,2})}{\sigma^2(\sigma^2 + \tau N_n(A_{L,2}))} \left(\frac{1}{n} \sum_{i:\mathbf{x}_i^{(1)} \in [c_1, c_2]} y_i^2 \right) \\
&\quad + \frac{\tau N_n(A_{L,2})}{\sigma^2(\sigma^2 + \tau N_n(A_{L,2}))} \left(\frac{1}{n} \sum_{i:\mathbf{x}_i^{(1)} \in [c_1, c_2]} (y_i - \bar{y}_{A_{L,2}})^2 \right) \\
&\quad - \frac{\tau N_n(A_{R,1})}{\sigma^2(\sigma^2 + \tau N_n(A_{R,1}))} \left(\frac{1}{n} \sum_{i:\mathbf{x}_i^{(1)} \in [c_1, c_2]} (y_i - \bar{y}_{A_{R,1}})^2 \right) \\
&= J_{21} + J_{22}.
\end{aligned}$$

Note that $|ax - by| \leq |a||x - y| + |a - b||y|$, we have

$$\begin{aligned}
|J_{22}| &= \left| \frac{\tau N_n(A_{L,2})}{\sigma^2(\sigma^2 + \tau N_n(A_{L,2}))} \left(\frac{1}{n} \sum_{i:\mathbf{x}_i^{(1)} \in [c_1, c_2]} (y_i - \bar{y}_{A_{L,2}})^2 \right) \right. \\
&\quad \left. - \frac{\tau N_n(A_{R,1})}{\sigma^2(\sigma^2 + \tau N_n(A_{R,1}))} \left(\frac{1}{n} \sum_{i:\mathbf{x}_i^{(1)} \in [c_1, c_2]} (y_i - \bar{y}_{A_{R,1}})^2 \right) \right| \\
&\leq \left| \frac{\tau N_n(A_{L,2})}{\sigma^2(\sigma^2 + \tau N_n(A_{L,2}))} \right| \times \left| \frac{1}{n} \sum_{i:\mathbf{x}_i^{(1)} \in [c_1, c_2]} (y_i - \bar{y}_{A_{L,2}})^2 - \frac{1}{n} \sum_{i:\mathbf{x}_i^{(1)} \in [c_1, c_2]} (y_i - \bar{y}_{A_{R,1}})^2 \right| \\
&\quad + \left| \frac{\tau N_n(A_{L,2})}{\sigma^2(\sigma^2 + \tau N_n(A_{L,2}))} - \frac{\tau N_n(A_{R,1})}{\sigma^2(\sigma^2 + \tau N_n(A_{R,1}))} \right| \times \left| \frac{1}{n} \sum_{i:\mathbf{x}_i^{(1)} \in [c_1, c_2]} (y_i - \bar{y}_{A_{R,1}})^2 \right|.
\end{aligned}$$

Since we assume that $c_1, c_2 \in A_{C, \sqrt{\delta}}$, by equation (19)

$$\begin{aligned}
\left| \frac{\tau N_n(A_{L,2})}{\sigma^2(\sigma^2 + \tau N_n(A_{L,2}))} \right| &\leq \left| \frac{\tau(\delta^2 - \sqrt{\delta})n}{\sigma^2(\sigma^2 + \tau(1 - \delta^2 - \sqrt{\delta})n)} \right| \\
&\leq \left| \frac{\tau(\delta^2 - \sqrt{\delta})}{\sigma^2(\tau(1 - \delta^2 - \sqrt{\delta}))} \right| \\
&= C(\delta) \rightarrow 0 \text{ as } \delta \rightarrow 0.
\end{aligned} \tag{21}$$

Note that this bound is valid for $N_n(A_{L,1}), N_n(A_{L,2}), N_n(A_{R,1})$ and $N_n(A_{R,2})$. By inequality (17) and (18), it is obvious that

$$\left| \frac{1}{n} \sum_{i: x_i^{(1)} \in [c_1, c_2]} (y_i - \bar{y}_{A_{R,1}})^2 \right| \leq \left| \frac{1}{N(A_C)} \sum_{i: x_i^{(1)} \in [c_1, c_2]} (y_i - \bar{y}_{A_{R,1}})^2 \right| \leq M$$

by a constant M . Furthermore

$$\left| \frac{\tau N_n(A_{L,2})}{\sigma^2(\sigma^2 + \tau N_n(A_{L,2}))} - \frac{\tau N_n(A_{R,1})}{\sigma^2(\sigma^2 + \tau N_n(A_{R,1}))} \right| \leq 2C(\delta). \tag{22}$$

The bound of second term follows equation (8) in supplementary materials of [Scornet et al. \(2015\)](#) directly,

$$|J_{22}| \leq C(\delta) \times 4(\|m\|_\infty + \alpha)((\delta + \delta^2)(2\|m\|_\infty + \alpha) + \alpha) + 2C(\delta)M.$$

The other term J_{21} is

$$\begin{aligned}
|J_{21}| &= \left| \frac{\tau N_n(A_{R,1})}{\sigma^2(\sigma^2 + \tau N_n(A_{R,1}))} \left(\frac{1}{n} \sum_{i: x_i^{(1)} \in [c_1, c_2]} y_i^2 \right) - \frac{\tau N_n(A_{L,2})}{\sigma^2(\sigma^2 + \tau N_n(A_{L,2}))} \left(\frac{1}{n} \sum_{i: x_i^{(1)} \in [c_1, c_2]} y_i^2 \right) \right| \\
&\leq \left| \frac{\tau N_n(A_{R,1})}{\sigma^2(\sigma^2 + \tau N_n(A_{R,1}))} - \frac{\tau N_n(A_{L,2})}{\sigma^2(\sigma^2 + \tau N_n(A_{L,2}))} \right| \times \left| \frac{1}{n} \sum_{i: x_i^{(1)} \in [c_1, c_2]} y_i^2 \right|.
\end{aligned}$$

The bound of coefficient here is slightly different from equation (21) and (22)

$$\begin{aligned}
& \left| \frac{\tau \mathbb{N}_n(A_{R,1})}{\sigma^2(\sigma^2 + \tau \mathbb{N}_n(A_{R,1}))} - \frac{\tau \mathbb{N}_n(A_{L,2})}{\sigma^2(\sigma^2 + \tau \mathbb{N}_n(A_{L,2}))} \right| \\
&= \left| \frac{\tau(\mathbb{N}_n(A_{R,1}) - \mathbb{N}_n(A_{L,2}))}{(\sigma^2 + \tau \mathbb{N}_n(A_{R,1}))(\sigma^2 + \tau \mathbb{N}_n(A_{L,2}))} \right| \\
&\leq \left| \frac{\tau}{(\sigma^2 + \tau \mathbb{N}_n(A_{R,1}))(\sigma^2 + \tau \mathbb{N}_n(A_{L,2}))} \right| (|\mathbb{N}_n(A_{R,1})| + |\mathbb{N}_n(A_{L,2})|) \\
&\leq \frac{2\tau(1 - \sqrt{\delta} + \delta^2)n}{(\sigma^2 + \tau(1 - \sqrt{\delta} - \delta^2)n)^2} = g(\delta, n) \rightarrow 0 \text{ when } n \text{ is large.}
\end{aligned} \tag{23}$$

Note that the upper bounds in equation (21) and (22) can be arbitrarily small if $\delta \rightarrow 0$, but the upper bound in equation (23) relies on making n large. Use the tail bound of non-central χ^2 distribution, result of supplementary materials of [Scornet et al. \(2015\)](#), and similar to J_{22}

$$|J_{21}| \leq g(\delta, n)M, \tag{24}$$

which can be arbitrarily small when n is large.

Now we switch to J_1 , corresponding to $i \mid \mathbf{x}_i^{(1)} \in [0, c_1]$, we proceed with similar decom-

position.

$$\begin{aligned}
J_1 &= \frac{\tau N_n(A_{L,1})}{\sigma^2(\sigma^2 + \tau N_n(A_{L,1}))} \frac{1}{n} \left(\sum_{i: x_i^{(1)} \leq c_1} y_i^2 - \sum_{i: x_i^{(1)} \leq c_1} (y_i - \bar{y}_{A_{L,1}})^2 \right) \\
&\quad - \frac{\tau N_n(A_{L,2})}{\sigma^2(\sigma^2 + \tau N_n(A_{L,2}))} \frac{1}{n} \left(\sum_{i: x_i^{(1)} \leq c_1} y_i^2 - \sum_{i: x_i^{(1)} \leq c_1} (y_i - \bar{y}_{A_{L,2}})^2 \right) \\
&= \frac{\tau N_n(A_{L,1})}{\sigma^2(\sigma^2 + \tau N_n(A_{L,1}))} \left(\frac{1}{n} \sum_{i: x_i^{(1)} \leq c_1} y_i^2 \right) - \frac{\tau N_n(A_{L,2})}{\sigma^2(\sigma^2 + \tau N_n(A_{L,2}))} \left(\frac{1}{n} \sum_{i: x_i^{(1)} \leq c_1} y_i^2 \right) \\
&\quad + \frac{\tau N_n(A_{L,2})}{\sigma^2(\sigma^2 + \tau N_n(A_{L,2}))} \left(\frac{1}{n} \sum_{i: x_i^{(1)} \leq c_1} (y_i - \bar{y}_{A_{L,2}})^2 \right) \\
&\quad - \frac{\tau N_n(A_{L,1})}{\sigma^2(\sigma^2 + \tau N_n(A_{L,1}))} \left(\frac{1}{n} \sum_{i: x_i^{(1)} \leq c_1} (y_i - \bar{y}_{A_{L,1}})^2 \right) \\
&= J_{11} + J_{12}.
\end{aligned}$$

$$\begin{aligned}
|J_{12}| &= \left| \frac{\tau N_n(A_{L,2})}{\sigma^2(\sigma^2 + \tau N_n(A_{L,2}))} \left(\frac{1}{n} \sum_{i: x_i^{(1)} \leq c_1} (y_i - \bar{y}_{A_{L,2}})^2 \right) \right. \\
&\quad \left. - \frac{\tau N_n(A_{L,1})}{\sigma^2(\sigma^2 + \tau N_n(A_{L,1}))} \left(\frac{1}{n} \sum_{i: x_i^{(1)} \leq c_1} (y_i - \bar{y}_{A_{L,1}})^2 \right) \right| \\
&\leq \left| \frac{\tau N_n(A_{L,2})}{\sigma^2(\sigma^2 + \tau N_n(A_{L,2}))} \right| \times \left| \frac{1}{n} \sum_{i: x_i^{(1)} \leq c_1} (y_i - \bar{y}_{A_{L,2}})^2 - \frac{1}{n} \sum_{i: x_i^{(1)} \leq c_1} (y_i - \bar{y}_{A_{L,1}})^2 \right| \\
&\quad + \left| \frac{\tau N_n(A_{L,2})}{\sigma^2(\sigma^2 + \tau N_n(A_{L,2}))} - \frac{\tau N_n(A_{L,1})}{\sigma^2(\sigma^2 + \tau N_n(A_{L,1}))} \right| \times \left| \frac{1}{n} \sum_{i: x_i^{(1)} \leq c_1} (y_i - \bar{y}_{A_{L,1}})^2 \right|.
\end{aligned}$$

Same as J_{22} ,

$$\begin{aligned} |J_{12}| &\leq C(\delta) \times \left| \frac{1}{n} \sum_{i: x_i^{(1)} \in [c_1, c_2]} (y_i - \bar{y}_{A_{R,1}})^2 \right| + 2C(\delta)M \\ &\leq C(\delta) \times 5(\|f\|_\infty \sqrt{\delta} + \alpha) + 2C(\delta)M. \end{aligned}$$

The second equation above use result of equation (9) of supplementary material of [Scornet et al. \(2015\)](#). Similar to J_{21} , we have

$$\begin{aligned} |J_{11}| &= \left| \frac{\tau N_n(A_{L,1})}{\sigma^2(\sigma^2 + \tau N_n(A_{L,1}))} \left(\frac{1}{n} \sum_{i: x_i^{(1)} \leq c_1} y_i^2 \right) - \frac{\tau N_n(A_{L,2})}{\sigma^2(\sigma^2 + \tau N_n(A_{L,2}))} \left(\frac{1}{n} \sum_{i: x_i^{(1)} \leq c_1} y_i^2 \right) \right| \\ &\leq \left| \frac{\tau N_n(A_{L,1})}{\sigma^2(\sigma^2 + \tau N_n(A_{L,1}))} - \frac{\tau N_n(A_{L,2})}{\sigma^2(\sigma^2 + \tau N_n(A_{L,2}))} \right| \times \left| \frac{1}{n} \sum_{i: x_i^{(1)} \leq c_1} y_i^2 \right| \\ &\leq g(\delta, n)M. \end{aligned}$$

J_3 have the same bound as J_1 . Collect all terms, we have

$$\begin{aligned} |J_1| &\leq g(\delta, n)M + C(\delta) \times 25(\|f\|_\infty \sqrt{\delta} + \alpha) + 2C(\delta)M \\ |J_2| &\leq g(\delta, n)M + C(\delta) \times 4(\|f\|_\infty + \alpha)((\delta + \delta^2)(2\|f\|_\infty + \alpha) + \alpha) + 2C(\delta)M \\ |J_3| &\leq g(\delta, n)M + C(\delta) \times 25(\|f\|_\infty \sqrt{\delta} + \alpha) + 2C(\delta)M \\ |L_{n,1}(1, c_1) - L_{n,1}(1, c_2)| &\leq |J_1| + |J_2| + |J_3| \end{aligned}$$

Consequently, for all n large enough and δ small enough, we have

$$|L_{n,1}(1, c_1) - L_{n,1}(1, c_2)| \leq 3\alpha.$$

Second case

Assume that $c_1, c_2 \in A_{L, \sqrt{\delta}}$, take same arguments as above, we have

$$N_n(A_{L,1}), N_n(A_{L,2}) \leq (\sqrt{\delta} + \delta^2)n.$$

Different from the first case, now both c_1 and c_2 are close to the left edge, which is corresponding to term J_1 . Note that $|J_2|$ and $|J_3|$ are the same as the first case since the control

over region A_C and $A_{R,1} \times A_{R,2}$ and not changed.

$$\begin{aligned}
|J_{12}| &= \left| \frac{\tau N_n(A_{L,2})}{\sigma^2(\sigma^2 + \tau N_n(A_{L,2}))} \left(\frac{1}{n} \sum_{i: x_i^{(1)} \leq c_1} (y_i - \bar{y}_{A_{L,2}})^2 \right) \right. \\
&\quad \left. - \frac{\tau N_n(A_{L,1})}{\sigma^2(\sigma^2 + \tau N_n(A_{L,1}))} \left(\frac{1}{n} \sum_{i: x_i^{(1)} \leq c_1} (y_i - \bar{y}_{A_{L,1}})^2 \right) \right| \\
&\leq \left| \frac{\tau N_n(A_{L,2})}{\sigma^2(\sigma^2 + \tau N_n(A_{L,2}))} \right| \times \left| \frac{1}{n} \sum_{i: x_i^{(1)} \leq c_1} (y_i - \bar{y}_{A_{L,2}})^2 - \frac{1}{n} \sum_{i: x_i^{(1)} \leq c_1} (y_i - \bar{y}_{A_{L,1}})^2 \right| \\
&\quad + \left| \frac{\tau N_n(A_{L,2})}{\sigma^2(\sigma^2 + \tau N_n(A_{L,2}))} - \frac{\tau N_n(A_{L,1})}{\sigma^2(\sigma^2 + \tau N_n(A_{L,1}))} \right| \times \left| \frac{1}{n} \sum_{i: x_i^{(1)} \leq c_1} (y_i - \bar{y}_{A_{L,1}})^2 \right|.
\end{aligned}$$

We have

$$\begin{aligned}
&\left| \frac{\tau N_n(A_{L,2})}{\sigma^2(\sigma^2 + \tau N_n(A_{L,2}))} \right| \leq \left| \frac{\tau N_n(A_{L,2})}{\sigma^2 \tau N_n(A_{L,2})} \right| = \frac{1}{\sigma^2} \\
&\left| \frac{1}{n} \sum_{i: x_i^{(1)} \leq c_1} (y_i - \bar{y}_{A_{L,2}})^2 - \frac{1}{n} \sum_{i: x_i^{(1)} \leq c_1} (y_i - \bar{y}_{A_{L,1}})^2 \right| \\
&= 2|\bar{y}_{A_{L,1}} - \bar{y}_{A_{L,2}}| \times \left| \frac{1}{n} \sum_{i: x_i^{(1)} < c_1} \left(y_i - \frac{\bar{y}_{A_{L,1}} + \bar{y}_{A_{L,2}}}{2} \right) \right| \\
&\leq 4(\|f\|_\infty + \alpha) \left(\frac{(\|f\|_\infty + \alpha) N_n(A_{L,1})}{n} + \frac{1}{n} \left| \sum_{i: x_i^{(1)} < c_1} f(x_i) + \epsilon_i \right| \right) \\
&\leq 4(\|f\|_\infty + \alpha) \left((\|f\|_\infty + \alpha)(\sqrt{\delta} + \delta^2) + \frac{N_n(A_{L,1})}{n} (\|f\|_\infty + \alpha) \right) \\
&\leq 4(\|f\|_\infty + \alpha) \left((\|f\|_\infty + \alpha + 1)(\sqrt{\delta} + \delta^2) \right)
\end{aligned}$$

$$\begin{aligned}
& \left| \frac{\tau N_n(A_{L,2})}{\sigma^2(\sigma^2 + \tau N_n(A_{L,2}))} - \frac{\tau N_n(A_{L,1})}{\sigma^2(\sigma^2 + \tau N_n(A_{L,1}))} \right| \times \left| \frac{1}{n} \sum_{i: x_i^{(1)} \leq c_1} (y_i - \bar{y}_{A_{L,1}})^2 \right| \\
&= \left| \frac{\tau N_n(A_{L,2})}{\sigma^2(\sigma^2 + \tau N_n(A_{L,2}))} - \frac{\tau N_n(A_{L,1})}{\sigma^2(\sigma^2 + \tau N_n(A_{L,1}))} \right| \times \frac{N_n(A_{L,1})}{n} \left| \frac{1}{N_n(A_{L,1})} \sum_{i: x_i^{(1)} \leq c_1} (y_i - \bar{y}_{A_{L,1}})^2 \right| \\
&\leq \frac{2}{\sigma^2} (\sqrt{\delta} + \delta^2) M.
\end{aligned}$$

As a result

$$|J_{12}| \leq \frac{1}{\sigma^2} 4(\|f\|_\infty + \alpha) \left((\|f\|_\infty + \alpha + 1)(\sqrt{\delta} + \delta^2) \right) + \frac{2}{\sigma^2} (\sqrt{\delta} + \delta^2) M \rightarrow 0.$$

$$\begin{aligned}
|J_{11}| &= \left| \frac{\tau N_n(A_{L,1})}{\sigma^2(\sigma^2 + \tau N_n(A_{L,1}))} \left(\frac{1}{n} \sum_{i: x_i^{(1)} \leq c_1} y_i^2 \right) - \frac{\tau N_n(A_{L,2})}{\sigma^2(\sigma^2 + \tau N_n(A_{L,2}))} \left(\frac{1}{n} \sum_{i: x_i^{(1)} \leq c_1} y_i^2 \right) \right| \\
&\leq \left| \frac{\tau N_n(A_{L,1})}{\sigma^2(\sigma^2 + \tau N_n(A_{L,1}))} - \frac{\tau N_n(A_{L,2})}{\sigma^2(\sigma^2 + \tau N_n(A_{L,2}))} \right| \times \left| \frac{1}{n} \sum_{i: x_i^{(1)} \leq c_1} y_i^2 \right| \\
&\leq \frac{2}{\sigma^2} (\sqrt{\delta} + \delta^2) M \rightarrow 0.
\end{aligned}$$

Consequently we conclude that for all $n > N$ and all δ small enough,

$$|L_{n,1}(1, c_1) - L_{n,1}(1, c_2)| \leq 3\alpha.$$

The other cases $\{c_1, c_2 \in A_{R, \sqrt{\delta}}\}$, $\{c_1 \in A_{L, \sqrt{\delta}}, c_2 \in A_{C, \sqrt{\delta}}\}$ and $\{c_1 \in A_{C, \sqrt{\delta}}, c_2 \in A_{R, \sqrt{\delta}}\}$ can be proved in the same way. Details are omitted.

B.2 Bounding strategy S2, Proof of Lemma 1 for the case $k = 2$

Next we prove S2, when adding variation to nodes above the parent of bottom nodes, the variation of split criterion is bounded. First, we assume $k = 2$.

Preliminary results

Similarly, [Laurent and Massart \(2000\)](#) gives tail bound of χ^2 distribution,

$$\mathbb{P}[\chi_n^2 \geq 5n] \leq \exp(-n).$$

By the tail bound above, it's straightforward to show that

Suppose X follows χ^2 distribution with degrees of freedom k and non-central parameter λ

$$P(X \geq x) \leq \frac{\sqrt{\pi}}{2e} \Phi(\sqrt{x}) I_{\frac{k}{2}}(1) M_{k-1},$$

where I_v is a modified Bessel function of the first kind, $M_{k-1} = E(y^{k-1})$ and y is a Gaussian $(\mu, 1)$ random variable truncated on (\sqrt{x}, ∞) . So we can claim that with probability $1 - \rho$, the term $\frac{1}{n} \sum_{i=1}^n y_i^2$ is bounded.

Follow the notation of [Scornet et al. \(2015\)](#), let $d'_1 = (1, c'_1)$ and $d'_2 = (2, x'_2)$ be such that $|c_1 - c'_1| \leq \delta$ and $|c_2 - x'_2| \leq \delta$.

There exist a constant $C_\rho > 0$ and N_1 such that, with probability $1 - \rho$, for all $n > N_1$,

$$\max_{1 \leq i \leq n} |\epsilon_i| \leq C_\rho \sqrt{\log(n)} \quad (25)$$

and

$$\max_{1 \leq i \leq n} |\epsilon_i^2| \leq C_\rho^2 \log(n). \quad (26)$$

Fix $\rho > 0$, there exist N_2 such that, with probability $1 - \rho$, for all $n > N_2$ and all $A_n = [a_n^{(1)}, b_n^{(1)}] \times [a_n^{(2)}, b_n^{(2)}] \subset [0, 1]^2$ satisfying $N_n(A_n) > \sqrt{n}$,

$$\left| \frac{1}{N_n(A_n)} \sum_{i: x_i \in A_n} \epsilon_i \right| \leq \alpha$$

and

$$\frac{1}{N_n(A_n)} \sum_{i: x_i \in A_n} \epsilon_i^2 \leq \tilde{\sigma}^2.$$

Furthermore, it's easy to verify

$$\left| \frac{1}{N_n(A_n)} \sum_{i: x_i \in A_n} y_i \right| \leq \|f\|_\infty + \alpha \quad (27)$$

and

$$\left| \frac{1}{N_n(A_n)} \sum_{i: x_i \in A_n} y_i^2 \right| \leq \|f\|_\infty^2 + \tilde{\sigma}^2 + 2\alpha \|f\|_\infty. \quad (28)$$

Similar to the $k = 1$ case, we denote partition of space as

$$\begin{cases} A_{R,1} = [c_1, 1] \times [0, 1]^{p-1} \\ A_{B,2} = [c_1, 1] \times [0, c_2] \times [0, 1]^{p-2} \\ A_{H,2} = [c_1, 1] \times [c_2, 1] \times [0, 1]^{p-2} \\ A'_{B,2} = [c'_1, 1] \times [0, c'_2] \times [0, 1]^{p-2} \\ A'_{H,2} = [c'_1, 1] \times [c'_2, 1] \times [0, 1]^{p-2}. \end{cases}$$

Figure 6 shows projection of the cells onto the first two variables.

Let $d_1 = (1, c_1)$ denotes cutpoint that splits at the first variable, value c_1 , similarly $d_2 = (2, c_2)$, $d'_1 = (1, c'_1)$ and $d'_2 = (2, c'_2)$ be four cutpoints and $|c_1 - c'_1| < \delta$, $|c_2 - c'_2| < \delta$, then

$$\begin{aligned} L_n(d_1, d_2) - L_n(d'_1, d'_2) &= L_n(d_1, d_2) - L_n(d'_1, d_2) \\ &\quad + L_n(d'_1, d_2) - L_n(d'_1, d'_2). \end{aligned} \quad (29)$$

It is noteworthy that equation (29) decomposes the variation to two terms, where the second term applies bounding strategies **S1** directly, and the first term is variation when the cutpoint of grandparent (two levels above bottom node) is perturbed.

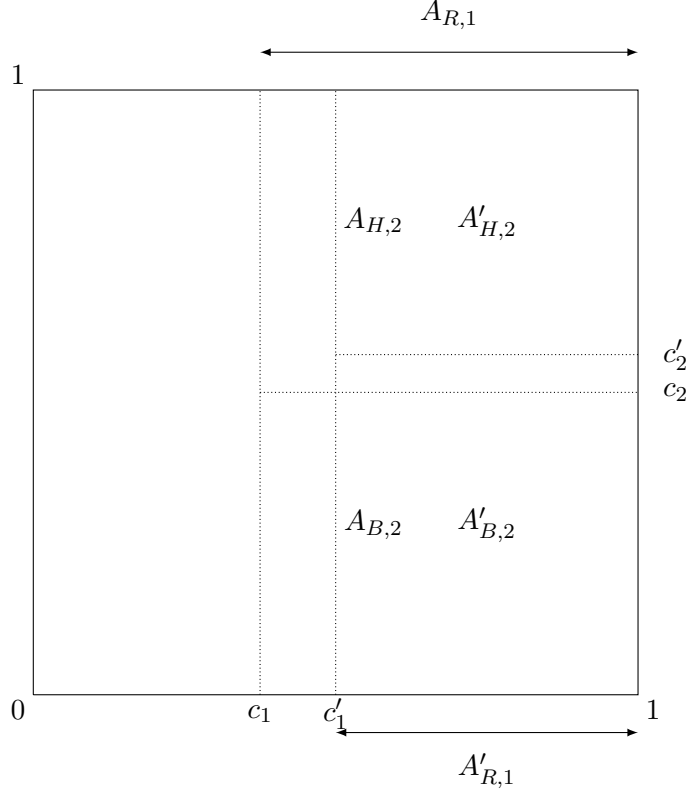


Figure 6: Illustration of notations for $k = 2$. Projection of cells onto the first two variables (assuming they are different variables).

$$\begin{aligned}
& L_n(d_1, d_2) - L_n(d'_1, d_2) \\
&= \frac{\tau N_n(A_{B,2})}{\sigma^2(\sigma^2 + \tau N_n(A_{B,2}))} \frac{1}{N_n(A_{R,1})} \left(\sum_{i: x_i^{(2)} \leq c_2} y_i^2 \mathbb{1}_{x_i^{(1)} > c_1} - \sum_{i: x_i^{(2)} \leq c_2} (y_i - \bar{y}_{A_{B,2}})^2 \mathbb{1}_{x_i^{(1)} > c_1} \right) \\
&\quad + \frac{\tau N_n(A_{H,2})}{\sigma^2(\sigma^2 + \tau N_n(A_{H,2}))} \frac{1}{N_n(A_{R,1})} \left(\sum_{i: x_i^{(2)} > c_2} y_i^2 \mathbb{1}_{x_i^{(1)} > c_1} - \sum_{i: x_i^{(2)} > c_2} (y_i - \bar{y}_{A_{H,2}})^2 \mathbb{1}_{x_i^{(1)} > c_1} \right) \\
&\quad - \frac{\tau N_n(A'_{B,2})}{\sigma^2(\sigma^2 + \tau N_n(A'_{B,2}))} \frac{1}{N_n(A'_{R,1})} \left(\sum_{i: x_i^{(2)} \leq c_2} y_i^2 \mathbb{1}_{x_i^{(1)} > c'_1} - \sum_{i: x_i^{(2)} \leq c_2} (y_i - \bar{y}_{A'_{B,2}})^2 \mathbb{1}_{x_i^{(1)} > c'_1} \right) \\
&\quad - \frac{\tau N_n(A'_{H,2})}{\sigma^2(\sigma^2 + \tau N_n(A'_{H,2}))} \frac{1}{N_n(A'_{R,1})} \left(\sum_{i: x_i^{(2)} > c_2} y_i^2 \mathbb{1}_{x_i^{(1)} > c'_1} - \sum_{i: x_i^{(2)} > c'_2} (y_i - \bar{y}_{A'_{H,2}})^2 \mathbb{1}_{x_i^{(1)} > c'_1} \right) \\
&\quad + \frac{\gamma_{c_1, c_2}}{N_n(A_{R,1})} - \frac{\gamma_{c'_1, c_2}}{N_n(A'_{R,1})} \\
&= A_1 + B_1
\end{aligned}$$

$$\begin{aligned}
A_1 &= \frac{\tau N_n(A_{H,2})}{\sigma^2(\sigma^2 + \tau N_n(A_{H,2}))} \frac{1}{N_n(A_{R,1})} \left(\sum_{i: x_i^{(2)} > c_2} y_i^2 \mathbf{1}_{x_i^{(1)} > c_1} - \sum_{i: x_i^{(2)} > c_2} (y_i - \bar{y}_{A_{H,2}})^2 \mathbf{1}_{x_i^{(1)} > c_1} \right) \\
&\quad - \frac{\tau N_n(A'_{H,2})}{\sigma^2(\sigma^2 + \tau N_n(A'_{H,2}))} \frac{1}{N_n(A'_{R,1})} \left(\sum_{i: x_i^{(2)} > c_2} y_i^2 \mathbf{1}_{x_i^{(1)} > c'_1} - \sum_{i: x_i^{(2)} > c'_2} (y_i - \bar{y}_{A'_{H,2}})^2 \mathbf{1}_{x_i^{(1)} > c'_1} \right) \\
&= A_{1,1} + A_{1,2} + A_{1,3}
\end{aligned}$$

$$\begin{aligned}
A_{1,1} &= \frac{\tau N_n(A_{H,2})}{\sigma^2(\sigma^2 + \tau N_n(A_{H,2}))} \frac{1}{N_n(A_{R,1})} \left(\sum_{i: x_i^{(2)} > c_2} y_i^2 \mathbf{1}_{x_i^{(1)} > c'_1} - \sum_{i: x_i^{(2)} > c_2} (y_i - \bar{y}_{A_{H,2}})^2 \mathbf{1}_{x_i^{(1)} > c'_1} \right) \\
&\quad - \frac{\tau N_n(A'_{H,2})}{\sigma^2(\sigma^2 + \tau N_n(A'_{H,2}))} \frac{1}{N_n(A_{R,1})} \left(\sum_{i: x_i^{(2)} > c_2} y_i^2 \mathbf{1}_{x_i^{(1)} > c'_1} - \sum_{i: x_i^{(2)} > c_2} (y_i - \bar{y}_{A'_{H,2}})^2 \mathbf{1}_{x_i^{(1)} > c'_1} \right)
\end{aligned}$$

$$\begin{aligned}
A_{1,2} &= \frac{\tau N_n(A'_{H,2})}{\sigma^2(\sigma^2 + \tau N_n(A'_{H,2}))} \frac{1}{N_n(A_{R,1})} \left(\sum_{i: x_i^{(2)} > c_2} y_i^2 \mathbf{1}_{x_i^{(1)} > c'_1} - \sum_{i: x_i^{(2)} > c_2} (y_i - \bar{y}_{A'_{H,2}})^2 \mathbf{1}_{x_i^{(1)} > c'_1} \right) \\
&\quad - \frac{\tau N_n(A'_{H,2})}{\sigma^2(\sigma^2 + \tau N_n(A'_{H,2}))} \frac{1}{N_n(A'_{R,1})} \left(\sum_{i: x_i^{(2)} > c_2} y_i^2 \mathbf{1}_{x_i^{(1)} > c'_1} - \sum_{i: x_i^{(2)} > c'_2} (y_i - \bar{y}_{A'_{H,2}})^2 \mathbf{1}_{x_i^{(1)} > c'_1} \right)
\end{aligned}$$

$$A_{1,3} = \frac{\tau N_n(A_{H,2})}{\sigma^2(\sigma^2 + \tau N_n(A_{H,2}))} \frac{1}{N_n(A_{R,1})} \left(\sum_{i: x_i^{(2)} > c_2} y_i^2 \mathbf{1}_{x_i^{(1)} \in [c_1, c'_1]} - \sum_{i: x_i^{(2)} > c_2} (y_i - \bar{y}_{A_{H,2}})^2 \mathbf{1}_{x_i^{(1)} \in [c_1, c'_1]} \right)$$

$$\begin{aligned}
A_{1,1} &= \frac{\tau N_n(A_{H,2})}{\sigma^2(\sigma^2 + \tau N_n(A_{H,2}))} \frac{1}{N_n(A_{R,1})} \left(\sum_{i: x_i^{(2)} > c_2} y_i^2 \mathbf{1}_{x_i^{(1)} > c'_1} - \sum_{i: x_i^{(2)} > c_2} (y_i - \bar{y}_{A_{H,2}})^2 \mathbf{1}_{x_i^{(1)} > c'_1} \right) \\
&\quad - \frac{\tau N_n(A'_{H,2})}{\sigma^2(\sigma^2 + \tau N_n(A'_{H,2}))} \frac{1}{N_n(A_{R,1})} \left(\sum_{i: x_i^{(2)} > c_2} y_i^2 \mathbf{1}_{x_i^{(1)} > c'_1} - \sum_{i: x_i^{(2)} > c_2} (y_i - \bar{y}_{A'_{H,2}})^2 \mathbf{1}_{x_i^{(1)} > c'_1} \right) \\
&= \left(\frac{\tau}{\sigma^2(\sigma^2 + \tau N_n(A_{H,2}))} \frac{N_n(A_{H,2})}{N_n(A_{R,1})} - \frac{\tau}{\sigma^2(\sigma^2 + \tau N_n(A'_{H,2}))} \frac{N_n(A'_{H,2})}{N_n(A_{R,1})} \right) \sum_{i: x_i^{(2)} > c_2} y_i^2 \mathbf{1}_{x_i^{(1)} > c'_1} \\
&\quad + \left(\frac{\tau}{\sigma^2(\sigma^2 + \tau N_n(A'_{H,2}))} \frac{N_n(A'_{H,2})}{N_n(A_{R,1})} \sum_{i: x_i^{(2)} > c_2} (y_i - \bar{y}_{A'_{H,2}})^2 \mathbf{1}_{x_i^{(1)} > c'_1} \right. \\
&\quad \left. - \frac{\tau}{\sigma^2(\sigma^2 + \tau N_n(A_{H,2}))} \frac{N_n(A_{H,2})}{N_n(A_{R,1})} \sum_{i: x_i^{(2)} > c_2} (y_i - \bar{y}_{A_{H,2}})^2 \mathbf{1}_{x_i^{(1)} > c'_1} \right)
\end{aligned}$$

which goes to zero using the same argument as $k = 1$ case.

$$\begin{aligned}
A_{1,2} &= \frac{\tau N_n(A'_{H,2})}{\sigma^2(\sigma^2 + \tau N_n(A'_{H,2}))} \frac{1}{N_n(A_{R,1})} \left(\sum_{i: x_i^{(2)} > c_2} y_i^2 \mathbf{1}_{x_i^{(1)} > c'_1} - \sum_{i: x_i^{(2)} > c_2} (y_i - \bar{y}_{A'_{H,2}})^2 \mathbf{1}_{x_i^{(1)} > c'_1} \right) \\
&\quad - \frac{\tau N_n(A'_{H,2})}{\sigma^2(\sigma^2 + \tau N_n(A'_{H,2}))} \frac{1}{N_n(A'_{R,1})} \left(\sum_{i: x_i^{(2)} > c_2} y_i^2 \mathbf{1}_{x_i^{(1)} > c'_1} - \sum_{i: x_i^{(2)} > c'_2} (y_i - \bar{y}_{A'_{H,2}})^2 \mathbf{1}_{x_i^{(1)} > c'_1} \right) \\
&= \left(\frac{\tau}{\sigma^2(\sigma^2 + \tau N_n(A'_{H,2}))} \frac{1}{N_n(A_{R,1})} - \frac{\tau}{\sigma^2(\sigma^2 + \tau N_n(A'_{H,2}))} \frac{1}{N_n(A'_{R,1})} \right) \\
&\quad \times \left(N_n(A'_{H,2}) \sum_{i: x_i^{(2)} > c_2} y_i^2 \mathbf{1}_{x_i^{(1)} > c'_1} - N_n(A'_{H,2}) \sum_{i: x_i^{(2)} > c_2} (y_i - \bar{y}_{A'_{H,2}})^2 \mathbf{1}_{x_i^{(1)} > c'_1} \right)
\end{aligned}$$

$$|A_{1,2}| \leq \left| \frac{\tau N_n(A'_{H,2})}{\sigma^2(\sigma^2 + \tau N_n(A'_{H,2}))} \frac{N_n(A'_{H,2})}{N_n(A_{R,1})} - \frac{\tau N_n(A'_{H,2})}{\sigma^2(\sigma^2 + \tau N_n(A'_{H,2}))} \frac{N_n(A'_{H,2})}{N_n(A'_{R,1})} \right| \\ \times \left(\left| \frac{1}{N_n(A'_{H,2})} \sum_{i: x_i^{(2)} > c_2} y_i^2 \mathbb{1}_{x_i^{(1)} > c'_1} \right| + \left| \frac{1}{N_n(A'_{H,2})} \sum_{i: x_i^{(2)} > c_2} (y_i - \bar{y}_{A'_{H,2}})^2 \mathbb{1}_{x_i^{(1)} > c'_1} \right| \right)$$

Same as before, the second term is bounded and

$$|A_{1,2}| \leq M \left| \frac{N_n(A'_{H,2})}{N_n(A_{R,1})} - \frac{N_n(A'_{H,2})}{N_n(A'_{R,1})} \right| \rightarrow 0$$

$$|A_{1,3}| \leq \left| \frac{\tau}{\sigma^2(\sigma^2 + \tau N_n(A_{H,2}))} \frac{N_n(A_{H,2})}{N_n(A_{R,1})} N_n(\{x_i^{(1)} \in [c_1, c'_1]\} \times \{x_i^{(2)} > c_2\}) \right| \\ \times \left| \frac{1}{N_n(\{x_i^{(1)} \in [c_1, c'_1]\} \times \{x_i^{(2)} > c_2\})} \sum_{i: x_i^{(2)} > c_2} y_i^2 \mathbb{1}_{x_i^{(1)} \in [c_1, c'_1]} \right| \\ + \left| \frac{\tau}{\sigma^2(\sigma^2 + \tau N_n(A_{H,2}))} \frac{N_n(A_{H,2})}{N_n(A_{R,1})} N_n(\{x_i^{(1)} \in [c_1, c'_1]\} \times \{x_i^{(2)} > c_2\}) \right| \\ \times \left| \frac{1}{N_n(\{x_i^{(1)} \in [c_1, c'_1]\} \times \{x_i^{(2)} > c_2\})} \sum_{i: x_i^{(2)} > c_2} (y_i - \bar{y}_{A_{H,2}})^2 \mathbb{1}_{x_i^{(1)} \in [c_1, c'_1]} \right| \\ = A_{1,3,1} + A_{1,3,2}.$$

Note that $\frac{\tau N_n(A_{H,2})}{\sigma^2(\sigma^2 + \tau N_n(A_{H,2}))}$ is bounded by a constant M as n is large,

$$\left| \frac{\tau}{\sigma^2(\sigma^2 + \tau N_n(A_{H,2}))} \frac{N_n(A_{H,2})}{N_n(A_{R,1})} N_n(\{x_i^{(1)} \in [c_1, c'_1]\} \times \{x_i^{(2)} > c_2\}) \right| \leq M \frac{\delta^2 + \delta}{\delta^2 - \sqrt{\delta}} \rightarrow 0.$$

So we have $A_{1,3,1} \rightarrow 0$ if n is large and δ is small.

If $N_n\left(\left\{x_i^{(1)} \in [c_1, c'_1]\right\} \times \left\{x_i^{(2)} > c_2\right\}\right) < \sqrt{n}$,

$$\left| \frac{1}{N_n\left(\left\{x_i^{(1)} \in [c_1, c'_1]\right\} \times \left\{x_i^{(2)} > c_2\right\}\right)} \sum_{l:x_i^{(2)} > c_2} (y_i - \bar{y}_{A_{H,2}})^2 \mathbf{1}_{x_i^{(1)} \in [c_1, c'_1]} \right| \leq \frac{C_\rho^2 \log(n)}{\sqrt{n}}.$$

If $N_n\left(\left\{x_i^{(1)} \in [c_1, c'_1]\right\} \times \left\{x_i^{(2)} > c_2\right\}\right) > \sqrt{n}$, note that $|1 - c_1| \geq \xi$, $N_n(A_{R,1}) > N_n(\xi) > (\xi - \delta^2)n$, $N_n\left(\left\{x_i^{(1)} \in [c_1, c'_1]\right\} \times \left\{x_i^{(2)} > c_2\right\}\right) \leq N_n\left(\left\{x_i^{(1)} \in [c_1, c'_1]\right\}\right) \leq (\delta + \delta^2)n$. As a result

$$\begin{aligned} & \left| \frac{N_n\left(\left\{x_i^{(1)} \in [c_1, c'_1]\right\} \times \left\{x_i^{(2)} > c_2\right\}\right)}{N_n(A_{R,1})} \right| \leq \frac{\delta - \delta^2}{\xi + \delta^2} \leq \frac{\delta}{\xi} \\ & \left| \frac{N_n\left(\left\{x_i^{(1)} \in [c_1, c'_1]\right\} \times \left\{x_i^{(2)} > c_2\right\}\right)}{N_n(A_{R,1})} \right| \\ & \quad \times \left| \frac{1}{N_n\left(\left\{x_i^{(1)} \in [c_1, c'_1]\right\} \times \left\{x_i^{(2)} > c_2\right\}\right)} \sum_{l:x_i^{(2)} > c_2} (y_i - \bar{y}_{A_{H,2}})^2 \mathbf{1}_{x_i^{(1)} \in [c_1, c'_1]} \right| \\ & \leq \frac{\delta}{\xi} (3(\|f\|_\infty + \alpha)^2 + \|f\|_\infty^2 + \tilde{\sigma}^2 + 2\|f\|_\infty^2 \alpha). \end{aligned}$$

Therefore $A_{1,3,2} \rightarrow 0$. Collecting all bounds, we conclude that $A_1 \rightarrow 0$. Bounding strategy **S1** proves that $B_1 \rightarrow 0$, thus we have $L_n(d_1, d_2) - L_n(d'_1, d'_2) \rightarrow 0$.

Remark Bounding strategy **S2** applies to perturbation at higher nodes as well. For example if we consider a sequence of three cutpoints $\mathbf{c}_3 = (d_1, d_2, d_3)$ and perturbation $\mathbf{c}'_3 = (d'_1, d'_2, d'_3)$. We can show that $L_n(d_1, d_2, d_3) - L_n(d'_1, d_2, d_3)$ is bounded using the same argument as **S2** since the second cutpoint d_2 is the same, and the cells can be projected on space spanned by variable 1 and 3 similarly as Figure 6.

B.3 Proof of Lemma 1 for the case $k > 2$

The proof for general $k > 2$ is based on the two bounding strategies **S1** and **S2** above. We scratch the essential ideas behind the proof in this section.

First, same as equation (20) and (29), we express the variation of split criterion as sum

of terms on one cutpoint at a time

$$\begin{aligned}
& L_{n,k}(d_1, d_2, \dots, d_{k-1}, d_k) - L_{n,k}(d'_1, d'_2, \dots, d'_{k-1}, d'_k) \\
& = L_{n,k}(d_1, d_2, \dots, d_{k-1}, d_k) - L_{n,k}(d'_1, d_2, \dots, d_{k-1}, d_k) \quad \mathbf{S2} \\
& + L_{n,k}(d'_1, d_2, \dots, d_{k-1}, d_k) - L_{n,k}(d'_1, d'_2, \dots, d_{k-1}, d_k) \quad \mathbf{S2} \\
& + \dots \\
& + L_{n,k}(d'_1, d'_2, \dots, d_{k-1}, d_k) - L_{n,k}(d'_1, d'_2, \dots, d'_{k-1}, d_k) \quad \mathbf{S2} \\
& + L_{n,k}(d'_1, d'_2, \dots, d'_{k-1}, d_k) - L_{n,k}(d'_1, d'_2, \dots, d'_{k-1}, d'_k) \quad \mathbf{S1}
\end{aligned} \tag{30}$$

Following remark in section [B.2](#), the first $k - 1$ terms are perturbation at cutpoints above the parent of bottom nodes (two levels above, or higher) and all cutpoints in between are fixed, therefore we can project cells to the variable being perturbed and the last cutpoint d_k similarly as in [Figure 6](#) and estimate bound. The last term is perturbation of the parent node of the bottom, therefore **S1** applies.